Title

CXCL10/CXCR3-Dependent Mobilization of Herpes Simplex Virus-Specific CD8+T$_{EM}$ and CD8+T$_{RM}$ Cells within Infected Tissues Allows Efficient Protection against Recurrent Herpesvirus Infection and Disease.

Authors

Srivastava, Ruchi
Khan, Arif A
Chilukuri, Sravya
et al.

Peer reviewed

![AMERICAN SOCIETY FOR MICROBIOLOGY | Journal of Virology®]

CXCL10/CXCR3-Dependent Mobilization of Herpes Simplex Virus-Specific CD8$^+$ T$_{EM}$ and CD8$^+$ T$_{RM}$ Cells within Infected Tissues Allows Efficient Protection against Recurrent Herpesvirus Infection and Disease

Ruchi Srivastava,[a] Arif A. Khan,[a] Sravya Chilukuri,[a] Sabrina A. Syed,[a] Tien T. Tran,[a] Julie Furness,[a] Elmostafa Bahraoui,[b,c] Lbachir BenMohamed[a,d,e]

Laboratory of Cellular and Molecular Immunology, Gavin Herbert Eye Institute, University of California Irvine, School of Medicine, Irvine, California, USA[a]; INSERM, U1043, and CNRS, U5282, Toulouse, France[b]; Université Paul Sabatier Toulouse, Toulouse, France[c]; Department of Molecular Biology and Biochemistry, University of California Irvine, Irvine, California, USA[d]; Institute for Immunology, University of California Irvine, School of Medicine, Irvine, California, USA[e]

ABSTRACT Herpes simplex virus 1 (HSV-1) establishes latency within the sensory neurons of the trigeminal ganglia (TG). HSV-specific memory CD8$^+$ T cells play a critical role in preventing HSV-1 reactivation from TG and subsequent virus shedding in tears that trigger recurrent corneal herpetic disease. The CXC chemokine ligand 10 (CXCL10)/CXC chemokine receptor 3 (CXCR3) chemokine pathway promotes T cell immunity to many viral pathogens, but its importance in CD8$^+$ T cell immunity to recurrent herpes has been poorly elucidated. In this study, we determined how the CXCL10/CXCR3 pathway affects TG- and cornea-resident CD8$^+$ T cell responses to recurrent ocular herpesvirus infection and disease using a well-established murine model in which HSV-1 reactivation was induced from latently infected TG by UV-B light. Following UV-B-induced HSV-1 reactivation, a significant increase in both the number and function of HSV-specific CXCR3$^+$ CD8$^+$ T cells was detected in TG and corneas of protected C57BL/6 (B6) mice, but not in TG and corneas of nonprotected CXCL10$^{-/-}$ or CXCR3$^{-/-}$ deficient mice. This increase was associated with a significant reduction in both virus shedding and recurrent corneal herpetic disease. Furthermore, delivery of exogenous CXCL10 chemokine in TG of CXCL10$^{-/-}$ mice, using the neurotropic adeno-associated virus type 8 (AAV8) vector, boosted the number and function of effector memory CD8$^+$ T cells (T$_{EM}$) and tissue-resident memory CD8$^+$ T cells (T$_{RM}$), but not of central memory CD8$^+$ T cells (T$_{CM}$), locally within TG, and improved protection against recurrent herpesvirus infection and disease in CXCL10$^{-/-}$ deficient mice. These findings demonstrate that the CXCL10/CXCR3 chemokine pathway is critical in shaping CD8$^+$ T cell immunity, locally within latently infected tissues, which protects against recurrent herpesvirus infection and disease.

IMPORTANCE We determined how the CXCL10/CXCR3 pathway affects CD8$^+$ T cell responses to recurrent ocular herpesvirus infection and disease. Using a well-established murine model, in which HSV-1 reactivation in latently infected trigeminal ganglia was induced by UV-B light, we demonstrated that lack of either CXCL10 chemokine or its CXCR3 receptor compromised the mobilization of functional CD8$^+$ T$_{EM}$ and CD8$^+$ T$_{RM}$ cells within latently infected trigeminal ganglia following virus reactivation. This lack of T cell mobilization was associated with an increase in recurrent ocular herpesvirus infection and disease. Inversely, augmenting the amount of

CXCL10 in trigeminal ganglia of latently infected CXCL10-deficient mice significantly restored the number of local antiviral CD8$^+$ T$_{EM}$ and CD8$^+$ T$_{RM}$ cells associated with protection against recurrent ocular herpes. Based on these findings, a novel "prime/pull" therapeutic ocular herpes vaccine strategy is proposed and discussed.

KEYWORDS CD8$^+$ T cells, CXCR3, CXCL10, herpes simplex virus, trigeminal ganglia, CD8, chemokine receptors, chemokines, immunization

A staggering 3.72 billion individuals worldwide (i.e., more than 52% of the world population) are currently infected with herpes simplex virus 1 (HSV-1), which causes a wide range of recurrent diseases throughout their lifetime (1–3). After the primary ocular HSV-1 infection, the virus establishes latency in sensory neurons of human trigeminal ganglia (TG), a state that lasts for the rest of the host's life (1, 4–6). Sporadic reactivation of the virus from latently infected sensory neurons of TG produces virus shedding in tears that can be either relatively asymptomatic or can cause significant corneal scarring and potentially blinding herpetic stromal keratitis (HSK) in symptomatic individuals (5–7). There are about 50,000 symptomatic recurrent cases of HSK every year in the United States. Current antiviral drug therapies (e.g., acyclovir and derivatives) reduce recurrent corneal disease by ~45% but do not eliminate virus reactivation from latently infected neurons of TG, which are the root of the disease (8, 9). An effective immunotherapeutic vaccine able to prevent HSV-1 reactivation from TG would be a powerful and cost-effective means to prevent viral shedding in tears and reduce recurrent corneal disease and blindness (reviewed in reference 10).

Following resolution of the primary infection, long-lived HSV-specific memory CD8$^+$ T cell populations are generated and provide protection against secondary infections (11, 12). These memory CD8$^+$ T cell populations are heterogeneous, but they can be divided into three major subpopulations: (i) the effector memory CD8$^+$ T cells (CD8$^+$ T$_{EM}$ cells), (ii) the central memory CD8$^+$ T cells (CD8$^+$ T$_{CM}$ cells), and (iii) the tissue-resident memory CD8$^+$ T cells (CD8$^+$ T$_{RM}$ cells) (13, 14). The TG-resident HSV-specific CD8$^+$ T cells play a crucial role in controlling HSV-1 reactivation from latently infected sensory neurons of TG (7, 15, 16). Chronic infiltrates of CD8$^+$ T cells surrounding HSV-1-infected neurons are present in human TG (17–22). An important goal in the development of an immunotherapeutic herpes vaccine is to increase the numbers of functional HSV-specific CD8$^+$ T cells in latently infected TG (23–26). This would prevent HSV-1 reactivation, stop or reduce virus shedding in the cornea, and cure recurrent herpetic disease. This task remains a major challenge, however, mainly because the TG tissue appears to be an "immunological closed compartment" inaccessible to circulating conventional CD8$^+$ T$_{CM}$ cells and CD8$^+$ T$_{EM}$ cells (27). Moreover, it is unclear whether a therapeutic vaccine would be able to boost TG-resident memory CD8$^+$ T$_{RM}$ cells (11, 14, 28, 29).

The chemokines CXCL9 (CXC chemokine ligand 9), CXCL10, and CXCL11, which exert their action via CXC chemokine receptor 3 (CXCR3), are considered crucial in directing CD8$^+$ T cells to sites of infection, such as the TG (13, 30, 31). Although these chemokines are known to potentiate T cell responses in the context of several viral infections (reviewed in reference 32), how they regulate herpes T cell immunity to herpesvirus reactivation from latency remains to be determined. Given the prominent expression of CXCL10 and CXCR3 in human TG (19), we investigated the role of the CXCL10/CXCR3 chemokine axis in shaping CD8$^+$ T$_{CM}$, CD8$^+$ T$_{EM}$, and CD8$^+$ T$_{RM}$ cell immunity against recurrent herpes. We report for the first time that UV-B induced HSV-1 reactivation from TG of latently infected wild-type C57BL/6 (B6) mice, but not from TG of mice deficient for CXCR3 or for CXCL10 (i.e., CXCR3$^{-/-}$ and CXCL10$^{-/-}$ mice), resulted in the following: (i) an increase in the number of HSV-specific CD8$^+$ T$_{EM}$ cells and CD8$^+$ T$_{RM}$ cells in the TG; (ii) an accumulation of polyfunctional cytotoxic and gamma interferon (IFN-γ)-producing CD8$^+$ T$_{EM}$ cells and CD8$^+$ T$_{RM}$ cells within latently infected TG; and (iii) a reduction in virus shedding in tears and a decrease in recurrent corneal herpetic disease. Furthermore, changing the immunological microenvironment of the latently

infected TG of CXCL10$^{-/-}$ deficient mice, following local delivery of neurotropic adeno-associated virus type 8 (AAV8) vector expressing CXCL10 chemokine, promoted the number and effector function of CD8$^+$ T$_{EM}$ cells and CD8$^+$ T$_{RM}$ cells in TG. This promotion was associated with a significant reduction in virus shedding and recurrent herpetic disease. These findings strongly suggest that the CXCL10/CXCR3 chemokine pathway plays a critical role in shaping antiviral CD8$^+$ T$_{EM}$ and CD8$^+$ T$_{RM}$ cell immunity against recurrent herpes. Based on these findings, a novel "prime/pull" therapeutic vaccine strategy to increase the number of functional CD8$^+$ T cells in latently infected TG is discussed.

RESULTS

Frequent HSV-specific CXCR3$^+$ CD3$^+$ CD8$^+$ T cells in trigeminal ganglia and cornea is associated with protection against virus shedding and recurrent ocular herpes disease. A group of 20 age- and sex-matched HLA-A*0201 transgenic mice (HLA Tg mice) were infected ocularly with 2×10^5 PFU of HSV-1 (strain McKrae) without corneal scarification as described in Materials and Methods. On day 24 (i.e., during the latent phase), the eyes of 15 infected animals that survived acute infection were exposed to UV-B irradiation in order to induce reactivation of HSV-1 from latently infected trigeminal ganglia (TG). UV-B irradiation led to virus shedding in tears and recurrent corneal herpetic disease, as we recently described (5, 6). The timeline of HSV-1 infection, UV-B irradiation, and subsequent immunological and virological assays is illustrated in Fig. 1A. During the 10 days following UV-B irradiation, virus shedding in tears was detected in ~60% of latently infected susceptible HLA Tg mice (BALB/c genetic background) (Fig. 1B), and ~80% developed apparent recurrent herpetic disease (Fig. 1A and C).

Subsequently, mice were segregated into two groups: protected mice with no recurrent corneal herpes disease (with the severity of disease scored below 1 on a scale of 0 to 4) and nonprotected mice with severe recurrent corneal herpetic disease (score of 2 to 4 on a scale of 0 to 4). On day 30 postinfection, protected and nonprotected HLA Tg mice were euthanized, and their corneas and TG were harvested for immunological assays. The percentages of cornea- and TG-resident CXCR3$^+$ CD8$^+$ T cells specific to the human HLA-A*0201-restricted HSV-1 epitope, VP11/12$_{220-228}$, were then compared for protected and nonprotected mice. As shown in Fig. 1D, significantly higher percentages of CXCR3$^+$ CD8$^+$ T cells specific to the immunodominant HSV-1 VP11/12$_{220-228}$ epitope were detected in the corneas and TG of protected mice compared to the corneas and TG of nonprotected mice (13.5% versus 2.7% and 7.5% versus 3.7%, respectively; $P < 0.05$). Moreover, increased levels of CXCR3 expression were detected on CD8$^+$ T cells in the corneas and TG of protected mice compared to nonprotected mice (Fig. 1E).

Altogether, these results indicate that frequent HSV-specific CXCR3$^+$ CD8$^+$ T cells present in the corneas and TG of protected mice compared to nonprotected mice are associated with less virus shedding in tears and less recurrent corneal herpetic disease. This suggests a potential role of the CXCR3 signaling pathway in mobilizing protective HSV-specific CD8$^+$ T cells into infected tissues.

CXCR3-dependent accumulation of functional CD103$^+$ CD8$^+$ T cells in the cornea and trigeminal ganglia is associated with a reduction of virus shedding in tears and prevention of recurrent corneal herpetic disease. We next determined whether the CXCR3 signaling pathway might also be crucial in the effector function of HSV-specific CD8$^+$ T cells in the cornea and TG. Since HLA Tg mice deficient for CXCR3 (i.e., CXCR3$^{-/-}$) are not available, we turned to the CXCR3-deficient mice that are available on the B6 genetic background and their wild-type (WT) B6 control littermates (33, 34). Both WT and CXCR3$^{-/-}$ deficient mice develop H2^b-restricted CD8$^+$ T cells specific to the immunodominant HSV-1 gB epitope (gB$_{498-505}$) following ocular infection with HSV-1.

A group of 20 age- and sex-matched WT B6 mice and 20 CXCR3$^{-/-}$ deficient mice were ocularly infected with 2×10^5 PFU of HSV-1 as described above and shown in Fig. 1A. On day 24 (i.e., during the latent phase), UV-B irradiation was used to induce virus
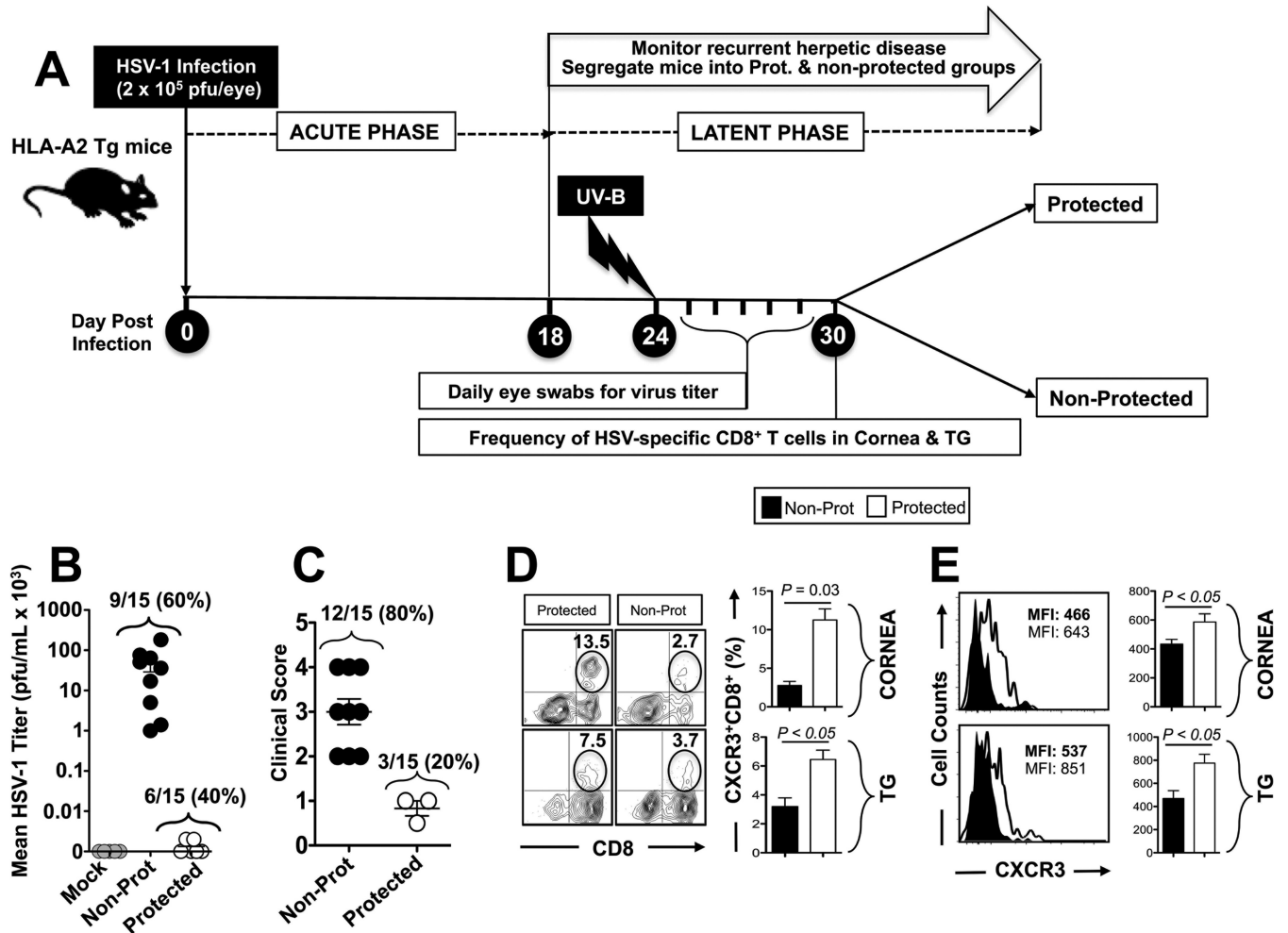
FIG 1 Trigeminal ganglia- and cornea-resident HSV-specific CXCR3+ CD8+ T cells are associated with protection against recurrent ocular herpesvirus infection and disease. A group of 20 HLA Tg mice (6 to 8 weeks old) were ocularly infected on day 0 with 2×10^5 PFU of HSV-1 (strain McKrae), as described in Materials and Methods. After establishment of latency (24 days postinfection), reactivation of latent virus was induced following irradiation with UV-B light. (A) Schematic representation of the time line of immunological and virological analyses in the UV-B mouse model of induced recurrent herpes. (B) Tears were collected daily for 10 days, and the presence of infectious virus in the tears was determined by plaque assay. The titer of virus detected in tear samples 6 days after UV-B irradiation was expressed as the mean virus load (in PFU per milliliter). (C) Recurrent corneal herpetic disease was monitored for up to 30 days after UV-B irradiation. Mice were observed daily for eye disease and clinically scored on a scale from 0 to 4. (D) Ten mice were euthanized on day 30 after UV-B exposure, and single-cell suspensions from corneas and TG were obtained after collagenase treatment, stained for markers of CXCR3+ CD3+ CD8+ T cells, and analyzed by FACS. Representative FACS plot of the frequency of VP11/12$_{220-228}$-specific CXCR3+ CD3+ CD8+ T cells detected in the corneas and TG of protected mice versus nonprotected (Non-Prot) mice. (E) Level of expression of CXCR3 receptor on CD8+ T cells from corneas and TG of protected mice versus nonprotected mice. The data are representative of two independent experiments. MFI, mean fluorescence intensity.

reactivation and recurrent corneal herpetic disease in both WT and CXCR3$^{-/-}$ mice that survive acute infection. We then compared the frequency of HSV-specific CD8+ T cells that accumulate in the corneas and TG of 10 WT B6 and CXCR3$^{-/-}$ mice 30 days following UV-B-induced reactivation. We also correlated the cytotoxic and IFN-γ productive functions of CD8+ T cells in TG and corneas of WT and CXCR3$^{-/-}$ mice with virus shedding and recurrent corneal herpetic disease following UV-B-induced reactivation.

Significantly higher percentages ($P < 0.05$) and numbers ($P = 0.04$) of CD103^{high} CD8+ T cells were detected in the TG of WT B6 mice compared to the TG of CXCR3$^{-/-}$ deficient mice (Fig. 2A and B). In contrast, there were slight, but nonsignificant, differences in the numbers of CD8+ T cells that were detected in the corneas of WT B6 mice compared to the corneas of CXCR3$^{-/-}$ deficient mice ($P > 0.05$; Fig. 2A and B).

As shown in Fig. 2C, UV-B-induced reactivation led to significantly more virus shedding in the eyes of CXCR3$^{-/-}$ deficient mice compared to WT B6 mice ($P = 0.03$).
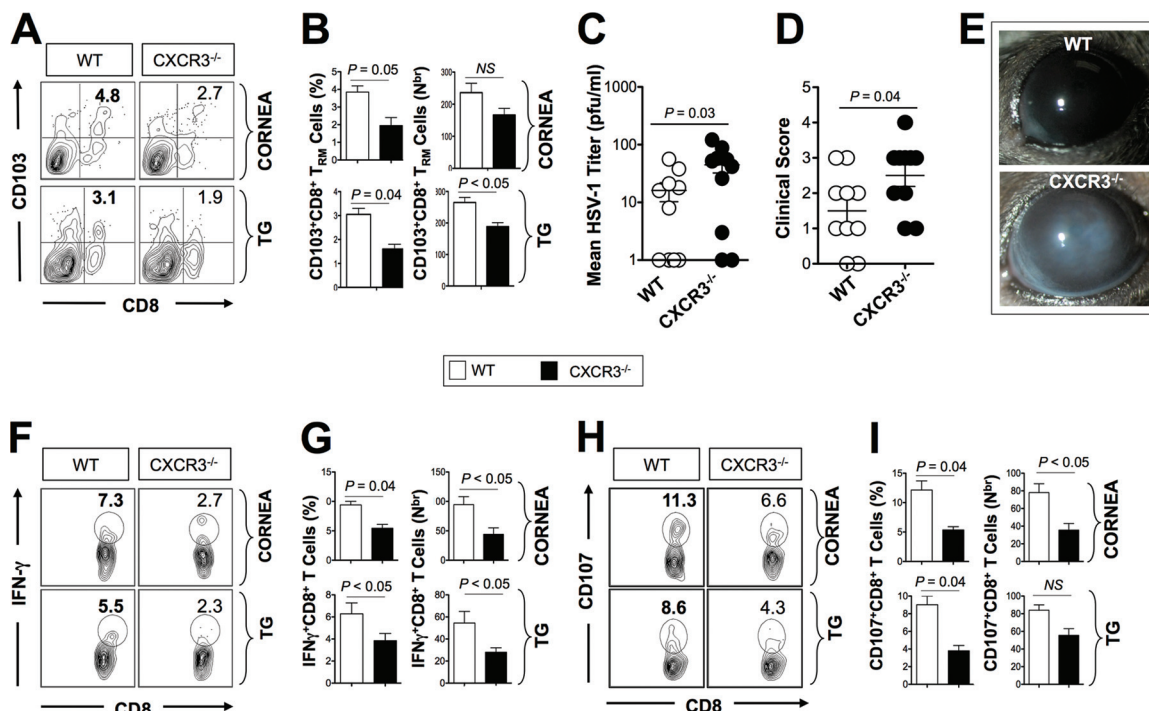
FIG 2 CXCR3$^{-/-}$ deficient mice developed less functional CD8$^+$ T cells in trigeminal ganglia and more recurrent corneal herpetic disease compared to wild-type (WT) B6 mice. A group of CXCR3$^{-/-}$ and WT mice (6 to 8 weeks old) were ocularly infected on day 0 with 2 × 10^5 PFU of HSV-1 (strain McKrae). After establishment of latency (24 days postinfection), reactivation of latent virus was induced after irradiation with UV-B. Tears were collected daily for 6 days after UV-B irradiation, and mice were euthanized on day 6 after UV-B exposure. Single-cell suspensions of corneas and TG were obtained after collagenase treatment and stained for markers of CD8$^+$ T$_{RM}$ cells, IFN-γ, and CD107, and analyzed by FACS. (A) Representative FACS plot of the frequency of HSV-specific CD8$^+$ T$_{RM}$ cells detected in the corneas and TG of WT and CXCR3$^{-/-}$ mice. (B) Average frequencies (left) and absolute numbers (right) of HSV-specific CD8$^+$ T$_{RM}$ cells detected in the corneas and TG of WT and CXCR3$^{-/-}$ mice. (C) Presence of infectious virus in the tears of WT and CXCR3$^{-/-}$ mice after UV-B treatment. The data are expressed as mean of virus load (in PFU per milliliter). (D) Mice were observed daily for eye disease and clinically scored from 0 to 4. (E) Representative slit lamp images of WT and CXCR3$^{-/-}$ mice corneas. (F and H) Representative FACS data of the frequencies of IFN-γ$^+$ CD8$^+$ T cells and CD107$^+$ CD8$^+$ T cells detected in the corneas and TG of WT and CXCR3$^{-/-}$ mice 6 days after UV-B exposure. (G and I) Average frequencies and absolute numbers of IFN-γ$^+$ CD8$^+$ T cells and CD107$^+$ CD8$^+$ T cells in the corneas and TG of WT and CXCR3$^{-/-}$ mice. The results are representative of two independent experiments. The indicated *P* values, calculated using unpaired *t* test, show statistical significance between WT and CXCR3$^{-/-}$ deficient mice. NS, not significant.

Moreover, during the 30 days following UV-B irradiation, 6 out of 10 CXCR3$^{-/-}$ deficient mice compared to only 2 out of 10 WT B6 mice developed severe corneal lesions with high scores of 3 and 4 ($P = 0.04$; Fig. 2D and E). On the other hand, the corneas and TG of CXCR3$^{-/-}$ deficient mice had significantly fewer IFN-γ-producing CD8$^+$ T cells compared to the corneas and TG of WT B6 mice ($P < 0.05$; Fig. 2F and G). Similarly, fewer CD107$^+$ CD8$^+$ T cells were detected in the corneas and TG of CXCR3$^{-/-}$ deficient mice compared to the corneas and TG of WT B6 mice ($P < 0.05$; Fig. 2H and I).

Altogether, these results demonstrate a crucial role of the CXCR3 signaling pathway in the mobilization and/or accumulation of IFN-γ-producing cytotoxic CD107$^+$ CD8$^+$ T cells in the cornea and TG. This suggests that higher mobilization and/or accumulation of IFN-γ-producing cytotoxic CD107$^+$ CD8$^+$ T cells is associated with control of UV-B-induced reactivation, less virus shedding, and less recurrent herpetic disease.

Increased recurrent ocular herpes is associated with reduced numbers of HSV-specific CD8$^+$ T$_{RM}$ and T$_{EM}$ cells in TG and corneas of latently infected CXCL10$^{-/-}$ deficient mice following UV-B-induced HSV-1 reactivation. We next determined the role of the CXCR3 signaling pathway in the mobilization and/or accumulation of the three major CD8$^+$ T cell subpopulations (i.e., CD8$^+$ T$_{EM}$ cells, CD8$^+$ T$_{CM}$ cells, and CD8$^+$ T$_{RM}$ cells) in the cornea and TG, in addition to their relative contribution in the observed protection against virus shedding and recurrent herpetic disease. Of the three T cell-attracting ligands of CXCR3 (i.e., CXCL9, CXCL10, and CXCL11), CXCL10 is the only chemokine that is predominantly expressed in human TG (19, 35). We therefore
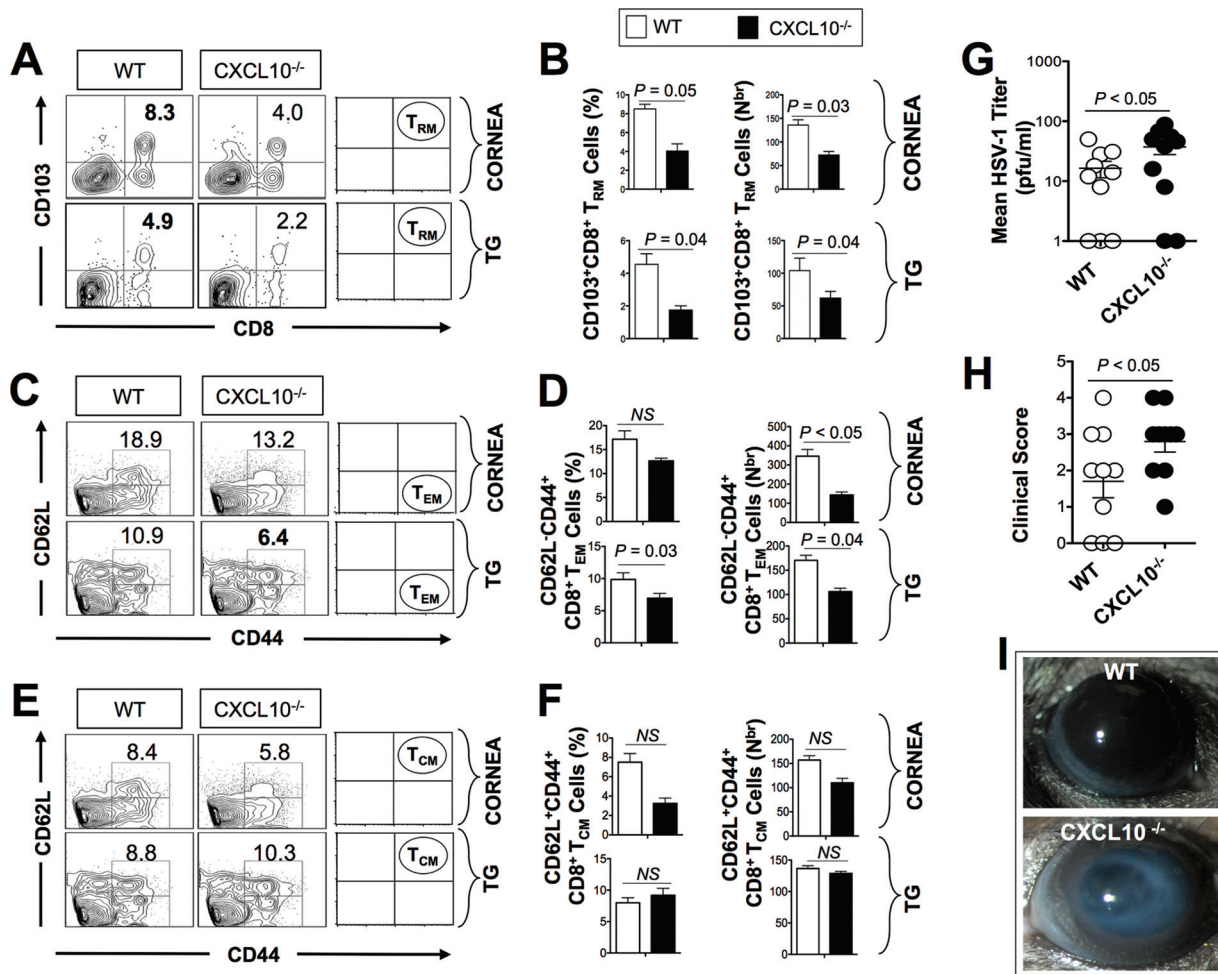
FIG 3 CXCL10$^{-/-}$ deficient mice have fewer HSV-specific CD8$^+$ T$_{RM}$ and T$_{EM}$ cells in the corneas and trigeminal ganglia and more virus shedding and more recurrent ocular herpetic disease compared to wild-type B6 mice. A group of CXCL10$^{-/-}$ and WT mice (6 to 8 weeks old) were ocularly infected on day 0 with 2×10^5 PFU of HSV-1 (strain McKrae) as described earlier. After establishment of latency (24 days postinfection), reactivation of latent virus was induced after irradiation with UV-B light. Ten mice were euthanized on day 30 after UV-B exposure, and single-cell suspensions from the corneas and TG were obtained after collagenase treatment at 37°C for an hour and stained for markers of CD8$^+$ T$_{RM}$, T$_{EM}$, and T$_{CM}$ cells and analyzed by FACS. (A, C, and E) Representative FACS plots of the frequency of HSV-specific CD8$^+$ T$_{RM}$ cells (A), CD8$^+$ T$_{EM}$ cells (C), and CD8$^+$ T$_{CM}$ cells (E) detected in the corneas and TG of WT and CXCL10$^{-/-}$ mice. (B, D, and F) Average percentages (left) and absolute numbers (right) of HSV-specific CD8$^+$ T$_{RM}$ cells (B), CD8$^+$ T$_{EM}$ cells (D), and CD8$^+$ T$_{CM}$ cells (F) detected in the corneas and TG of WT and CXCL10$^{-/-}$ mice. (G) Viral titer estimation detected in tear samples 6 days after UV-B irradiation expressed as mean of virus load (in PFU per milliliter). (H and I) Recurrent corneal herpetic disease was monitored for up to 30 days after UV-B irradiation. Mice were observed daily for eye disease and clinically scored on a scale of 0 to 4. The results are representative of two independent experiments. The indicated P values, calculated using unpaired t test, show statistical significance between WT and CXCL10$^{-/-}$ deficient mice. NS, not significant.

investigated whether lack of the CXCL10 chemokine would affect the mobilization and/or accumulation and effector function of CD8$^+$ T$_{EM}$ cells, CD8$^+$ T$_{CM}$ cells, and CD8$^+$ T$_{RM}$ cells in the cornea and TG following UV-B-induced reactivation.

A group of 20 sex- and age-matched CXCL10-deficient mice (CXCL10$^{-/-}$) and 20 WT B6 control littermates were infected ocularly on day 0 with 2×10^5 PFU of HSV-1 without corneal scarification as described in Materials and Methods. On day 24 (i.e., during the latent phase), UV-B irradiation was used to induce virus reactivation in surviving latently infected animals as described above.

Following UV-B reactivation, significantly lower percentages (Fig. 3A and B, left) and numbers (Fig. 3B, right) of CD103^{high} CCR7^{low} CD11a^{high} CD69^{high} CD8$^+$ T$_{RM}$ cells were detected in the corneas and TG of CXCL10$^{-/-}$ mice than in the corneas and TG of WT mice ($P = 0.05$ for the cornea and $P = 0.04$ for the TG). Similarly, a significantly lower percentage (Fig. 3C and D, left; $P = 0.03$) and number (Fig. 3D, right; $P = 0.04$) of CD44^{high} CD62L^{low} CD8$^+$ T$_{EM}$ cells were detected in TG of CXCL10$^{-/-}$ mice compared

to TG of WT mice. However, no significant differences in the frequencies of CD44^{high} CD62L^{high} CD8$^+$ T$_{CM}$ cells were detected in the corneas and TG of CXCL10$^{-/-}$ mice compared to the corneas and TG of WT mice (Fig. 3E and F, left; $P > 0.05$).

Moreover, as shown in Fig. 3G, UV-B-induced reactivation led to significantly more virus shedding in the eyes of CXCL10$^{-/-}$ deficient mice compared to WT B6 mice ($P < 0.05$). During the 30 days following UV-B irradiation, 7 out of 10 CXCL10$^{-/-}$ deficient mice compared to only 3 out of 10 WT B6 mice developed severe corneal lesions with high scores of 3 and 4 ($P = 0.04$; Fig. 3H and I).

These results point to a pivotal role of the CXCR3/CXCL10 signaling pathway in the mobilization and/or accumulation of antiviral CD8$^+$ T$_{EM}$ cells and CD8$^+$ T$_{RM}$ cells, but not CD8$^+$ T$_{CM}$ cells, in the cornea and TG following UV-B-induced reactivation. These results indicate that the failure to contain recurrent corneal herpetic infection and disease in CXCL10$^{-/-}$ deficient mice positively correlated with the loss of cornea- and TG-resident CD8$^+$ T$_{EM}$ cells and CD8$^+$ T$_{RM}$ cells, but not CD8$^+$ T$_{CM}$ cells. These results suggest a crucial role of CD8$^+$ T$_{EM}$ cells and CD8$^+$ T$_{RM}$ cells, but not CD8$^+$ T$_{CM}$ cells, in protection against virus shedding and recurrent herpetic disease.

More dysfunctional VISTA$^+$ PD-1$^+$ CD8$^+$ T cells are present in the TG and corneas of latently infected CXCL10$^{-/-}$ deficient mice than in wild-type B6 mice. A group of 20 sex- and age-matched CXCL10-deficient mice (CXCL10$^{-/-}$) and 20 WT B6 control littermates were infected ocularly on day 0 with 2×10^5 PFU of HSV-1 as described above. Ten days after UV-B-induced reactivation, the function and dysfunction of CD8$^+$ T cells in the corneas and TG of 10 randomly picked CXCL10$^{-/-}$ deficient mice and 10 WT mice were analyzed using several markers of immunological function and dysfunction. These markers included the production of antiviral IFN-γ, CD107$^{a/b}$ cytotoxic degranulation, and expression of markers of exhaustion, including programmed cell death protein 1 (also known as PD-1), T cell immunoreceptor with Ig and ITIM domains (also known as TIGIT), the V-domain Ig suppressor of T cell activation (also known as VISTA, 2B4, and Tim-3) (36–38).

As shown in Fig. 4A and B, following UV-B-induced reactivation, significantly low numbers of IFN-γ-producing CD8$^+$ T cells were detected in the corneas and TG of CXCL10$^{-/-}$ deficient mice compared to B6 mice ($P < 0.05$). The percentage and number of IFN-γ producing CD8$^+$ T cells were reduced approximately twofold in TG of CXCL10$^{-/-}$ mice compared to TG of WT B6 mice. There is also a significant reduction of cytotoxic CD107$^+$ CD8$^+$ T cells in the corneas and TG of CXCL10$^{-/-}$ deficient mice compared to the corneas and TG of B6 mice ($P < 0.05$; Fig. 4C and D).

As shown in Fig. S1 in the supplemental material, following UV-B-induced reactivation, significantly less functional TNF-α-producing CD8$^+$ T cells were detected in both the corneas and TG of CXCL10$^{-/-}$ deficient mice compared to the corneas and TG of B6 mice ($P < 0.05$). Similarly, significantly lower expression of GzmB and EOMES were detected on CD8$^+$ T cells from both the corneas and TG of CXCL10$^{-/-}$ deficient mice compared to the corneas and TG of B6 mice ($P < 0.05$). In contrast, significantly lower T-bet expression was detected only on CD8$^+$ T cells from TG of CXCL10$^{-/-}$ deficient mice compared to TG of B6 mice ($P < 0.05$).

Furthermore, as shown in Fig. 4E and F, there was an approximately twofold increase in the percentage and number of VISTA$^+$ CD8$^+$ T cells in the corneas and TG of CXCL10$^{-/-}$ mice compared to the corneas and TG of WT B6 mice. A significant increase in the percentage of PD-1$^+$ CD8$^+$ T cells was also detected in the corneas and TG of CXCL10$^{-/-}$ mice compared to the corneas and TG of WT B6 mice ($P < 0.05$; Fig. 4G and H). CXCL10$^{-/-}$ mice also exhibited higher frequencies of Tim-3$^+$ CD8$^+$ T cells, 2B4$^+$ CD8$^+$ T cells, and TIGIT$^+$ CD8$^+$ T cells in corneas and TG compared to WT mice (Fig. S2; $P < 0.05$).

Altogether, these results suggest that the lack of CXCL10 chemokine is associated with the following: (i) a significant impairment in the effector functions of CD8$^+$ T cells (antiviral IFN-γ and CD107$^{a/b}$ cytotoxic degranulation) in both the corneas and TG of CXCL10$^{-/-}$ deficient mice; and (ii) a significant increase in exhausted PD-1$^+$ CD8$^+$, TIGIT$^+$ CD8$^+$, Tim-3$^+$ CD8$^+$, 2B4$^+$ CD8$^+$, and VISTA$^+$ CD8$^+$ T cells in the corneas and
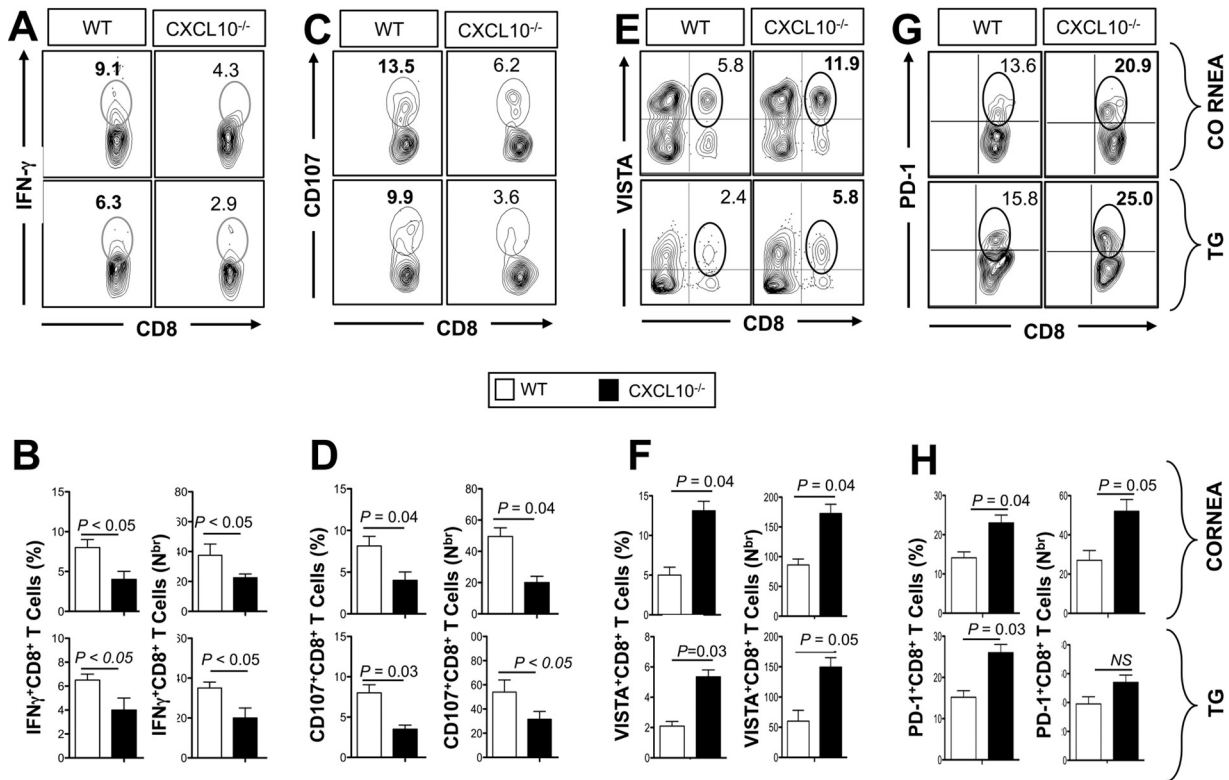
FIG 4 More dysfunctional CD8+ T cells are present in the corneas and trigeminal ganglia of CXCL10−/− deficient mice compared to the corneas and trigeminal ganglia of wild-type B6 mice. HSV-1 latently infected WT and CXCL10−/− mice (n = 10) were euthanized 6 days after UV-B exposure. Single-cell suspensions from corneas and TG were obtained after collagenase treatment at 37°C and stained for IFN-γ, CD107, VISTA, and PD-1 and analyzed by FACS. (A, C, E, and G) Representative FACS plots of the frequency of HSV-specific IFN-γ+ CD8+ T cells (A), CD107+ CD8+ T cells (C), VISTA+ CD8+ T cells (E), and PD-1+ CD8+ T cells (G) detected in the corneas and TG of WT and CXCL10−/− mice. (B, D, F, and H) Average percentages (left) and absolute numbers (right) of HSV-specific IFN-γ+ CD8+ T cells (B), CD107+ CD8+ T cells (D), VISTA+ CD8+ T cells (F), and PD-1+ CD8+ T cells (H) detected in the corneas and TG of WT and CXCL10−/− mice. The results are representative of two independent experiments. The indicated P values, calculated using unpaired t test, show statistical significance between WT and CXCL10−/− deficient mice.

TG of CXCL10−/− deficient mice. Beside the reduced number of antiviral CD8+ T_EM and T_RM cells in the corneas and TG of CXCL10−/− deficient mice, the reduced function and increased dysfunction of these CD8+ T cells may further contribute to the enhanced susceptibility to recurrent ocular herpetic infection and disease observed in CXCL10−/− deficient mice following virus reactivation. The results confirm a pivotal role of the CXCR3/CXCL10 signaling pathway in the antiviral CD8+ T cell immunity in the cornea and TG following virus reactivation.

Topical ocular application of neurotropic AAV8 vectors expressing CXCL10, but not CXCL9, chemokine promotes the protective function of antiviral CD8+ T_RM cells and CD8+ T_EM cells in the trigeminal ganglia of CXCL10−/− mice. We next determined whether correcting the apparent deficiency of CXCL10 chemokine in the TG of CXCL10−/− deficient mice would increase the number of CD8+ T cells in TG, reverse their dysfunction, and rescue their protective function. We used the neurotropic recombinant adeno-associated virus type 8 (rAAV8) vector that expresses CXCL10 chemokine locally in latently infected TG under the neurotropic calcium/calmodulin-dependent protein kinase type II subunit alpha (CamKII-α) promoter.

As illustrated in Fig. 5, CXCL10−/− mice (n = 20) were infected with HSV-1 on day 0, and the eyes of all animals were exposed on day 24 to UV-B irradiation in order to induce virus reactivation as described above. On day 30, half of the animals received topical application of 1×10^7 PFU/eye of a neurotropic recombinant rAAV8 expressing either CXCL10 or CXCL9 mouse chemokine together with green fluorescent protein (GFP), both under the neurotropic CamKII-α promoter (i.e., rAAV8-CXCL9 or rAAV8-CXCL10 [Fig. 5B]). Following topical application of rAAV8-CXCL10, the GFP protein
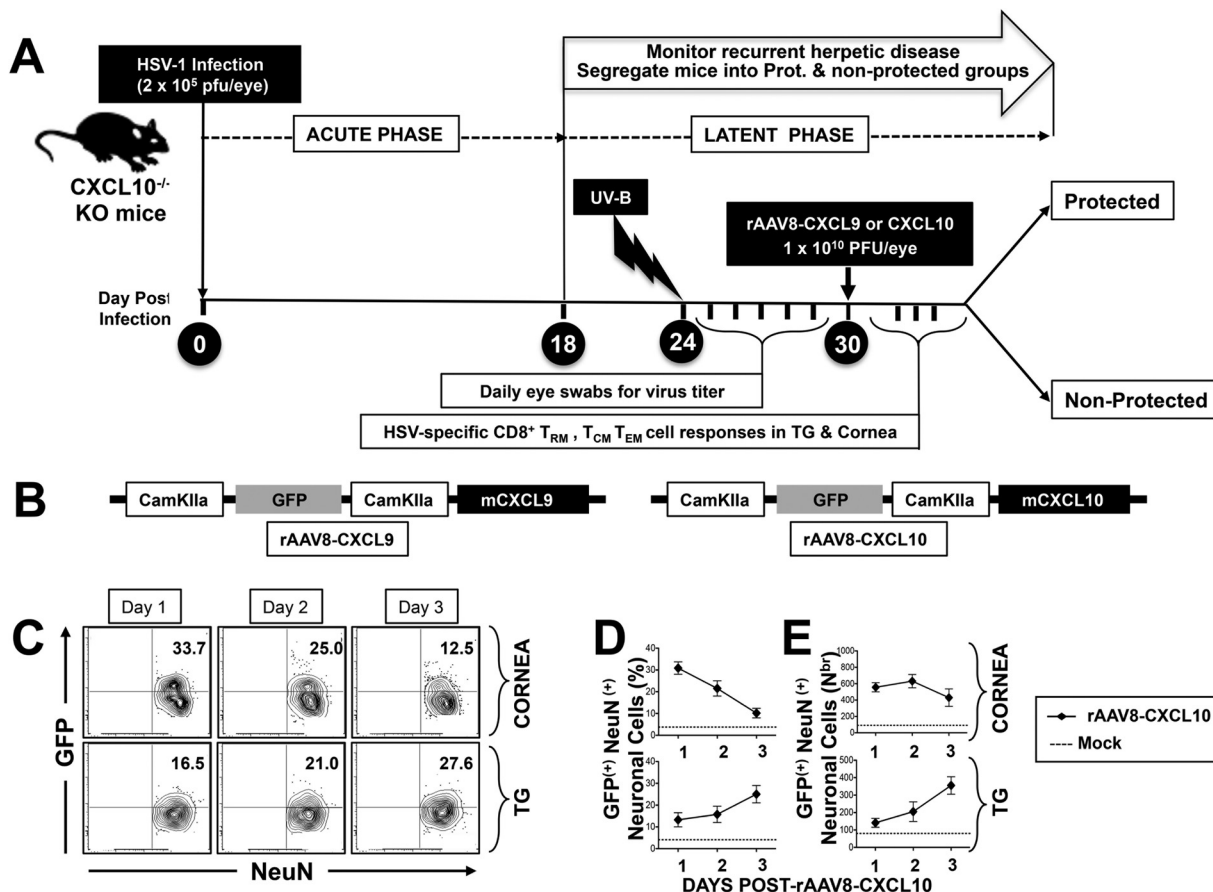
FIG 5 Coexpression of a neurotropic recombinant adeno-associated virus type 8 (fAAV8) bearing GFP and CXCL10 chemokine in latently infected trigeminal ganglia of CXCL10$^{-/-}$ mice following topical ocular application. CXCL10$^{-/-}$ mice ($n = 20$) were ocularly infected using 2×10^5 wild-type McKrae (HSV-1) strain. Twenty-four days postinfection, when latency was fully established, animals were exposed to UV-B irradiation to induce virus reactivation. On day 30, half of the animals ($n = 10$) received topical application of 1×10^7 PFU/eye of a neurotropic recombinant adeno-associated virus type 8 expressing either CXCL9 or CXCL10 mouse chemokine together with GFP, both under the neurotropic CamKII-α promoter. The other half of the animals ($n = 10$) received topical application of 1×10^7 PFU/eye of an AAV8 empty vector (Mock). Mice were euthanized on day 1, day 2, and day 3 after rAAV8-CXCL9 or rAAV8-CXCL10 treatment. (A) Schematic representation of the time line of HSV-1 infection and rAAV8-CXCL9 and rAAV8-CXCL10 treatment in the UV-B-CXCL10$^{-/-}$ mouse model. KO, knockout. (B) Structure of recombinant AAV vector bearing the T cell-attracting chemokine CXCL9 or CXCL10 tagged with GFP with both chemokines expressed under the CamKII-α promoter. (C) Representative FACS plot of the frequency of NeuN$^+$ neuronal cells expressing GFP in cornea and TG, detected on days 1, 2, and 3 after rAAV8-CXCL10 treatment, in corneas and TG of CXC10$^{-/-}$ mice. (D) Average frequencies (left) and absolute number (right) of NeuN$^+$ neuronal cells expressing GFP in cornea and TG, detected on days 1, 2, and 3 after rAAV8-CXCL10 treatment, in the corneas and TG of CXC10$^{-/-}$ mice. The data are representative of two independent experiments. The indicated P values, calculated using unpaired t test, show statistical significance between CXCL10-treated and untreated mice.

expression was detected by fluorescence-activated cell sorting (FACS) in NeuN$^+$ neuronal cell suspensions from both the corneas and TG of CXCL10$^{-/-}$ deficient mice within 1 day (Fig. 5C to E). While GFP expression decreased in the cornea over 3 days, its expression gradually increased in TG over time.

Moreover, a significant increase in CD8$^+$ T cells was detected by immunostaining in TG of CXCL10$^{-/-}$ mice following UV-B-induced reactivation and topical ocular application of rAAV8-CXCL10 compared to TG of untreated CXCL10$^{-/-}$ mice (Fig. 6A). We next determined whether treatment with rAAV8-CXCL10 resulted in the mobilization and/or accumulation of the three major CD8$^+$ T cell subpopulations (i.e., CD8$^+$ T$_{EM}$ cells, CD8$^+$ T$_{CM}$ cells, and CD8$^+$ T$_{RM}$ cells) in TG and their relative contribution in the protection against recurrent herpetic disease following UV-B-induced reactivation. We used FACS analysis to quantify the three CD8$^+$ T cell subpopulations in TG of rAAV8-CXCL10-treated and untreated CXCL10$^{-/-}$ mice.

Topical ocular application of rAAV8-CXCL10 was associated with a significant increase in the percentage and number of CD103$^+$ CD8$^+$ T$_{RM}$ cells (Fig. 6B and C)
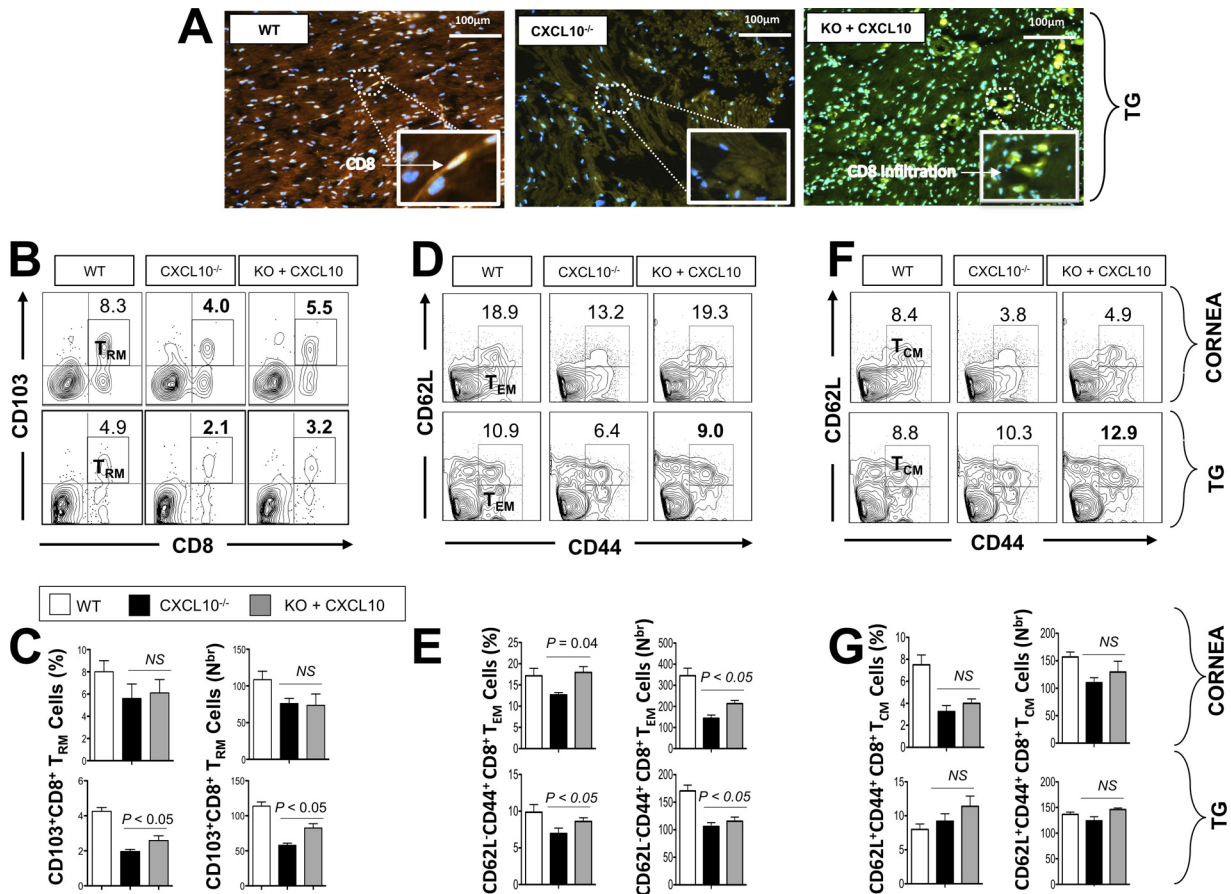
FIG 6 Topical ocular application of neurotropic AAV8 vector expressing CXCL10 increased the number of CD8⁺ T_RM and T_EM cells in the corneas and trigeminal ganglia of latently infected CXCL10⁻/⁻ mice. Wild-type B6 mice ($n = 10$) and CXCL10⁻/⁻ mice ($n = 20$) were ocularly infected using 2×10^5 wild-type McKrae (HSV-1) strain. At 24 days postinfection, when latency was fully established, reactivation of latent HSV-1 infection was induced after UV-B irradiation. Six days after UV-B irradiation, half of CXCL10⁻/⁻ mice ($n = 10$) received topical application of 1×10^7 PFU/eye of a neurotropic rAAV8 expressing either CXCL10 chemokine. The other half of the animals ($n = 10$) received topical application of 1×10^7 PFU/eye of an AAV8 empty vector. (A) TG sections from WT and CXCL10⁻/⁻ mice were costained using a MAb specific to CD8⁺ T cells or to neurons, together with GFP. For the wild-type B6 mice, PE-labeled CXCL10 (red), 4′,6′-diamidino-2-phenylindole (DAPI) (DNA stain) (blue), and CD8 infiltration orange color (yellow) are indicated. For the CXCL10⁻/⁻ mice, PE-labeled CXCL10 (red), DAPI (blue), and CD8⁺ T cells (yellow) are indicated. For the CXCL10⁻/⁻ mice 3 days after rAAV8-CXCL10 treatment, CXCL10 (red), DAPI (blue), CD8⁺ cells (yellow) and GFP (green) are indicated. Single-cell suspensions from corneas and TG were obtained after collagenase treatment at 37°C for an hour and stained for markers of CD8⁺ T_RM cells, IFN-γ, and CD107a/b and analyzed by FACS. CXCL10⁻/⁻ mice were euthanized on day 30 after UV-B exposure, and single-cell suspensions from the corneas and TG were obtained after collagenase treatment at 37°C for an hour and stained for markers of CD8⁺ T_RM, T_EM, and T_CM cells and analyzed by FACS. (B, D, and F) Representative FACS plots of the frequencies of HSV-specific CD8⁺ T_RM cells (B), CD8⁺ T_EM cells (D), and CD8⁺ T_CM cells (F) detected in the cornea and TG of WT mice (left), untreated CXCL10⁻/⁻ mice (middle), and CXCL10⁻/⁻ mice treated with rAAV8-CXCL10 (right). (C, E, and G) Average percentages (left) and absolute numbers (right) of HSV-specific CD8⁺ T_RM cells (C), CD8⁺ T_EM cells (E), and CD8⁺ T_CM cells (G) detected in the corneas and TG of WT and CXCL10⁻/⁻ mice untreated and treated with rAAV8-CXCL10. The data are representative of two independent experiments. The indicated P values were calculated using one-way ANOVA and pairwise multiple comparisons were performed stratified by experiment. Bonferroni correction was utilized to adjust the multiple comparisons. SAS v.9.4 (Statistical Analysis System, Cary, NC) was used. Graphs were prepared with GraphPad Prism software (San Diego, CA). Data are expressed as the mean + SD. Error bars show SEM.

detected in TG of rAAV8-CXCL10-treated CXCL10⁻/⁻ mice compared to TG of untreated CXCL10⁻/⁻ mice ($P < 0.05$ for the cornea and $P = 0.04$ for the TG). Similarly, a significantly lower percentage (Fig. 6D and E, left; $P = 0.04$) and number (Fig. 6E, right; $P < 0.05$) of CD44^high CD62L^low CD8⁺ T_RM cells were detected in TG of rAAV8-CXCL10-treated CXCL10⁻/⁻ mice compared to TG of untreated CXCL10⁻/⁻ mice. However, no significant differences in the frequencies of CD44^high CD62L^high CD8⁺ T_CM cells were detected in the corneas and TG of rAAV8-CXCL10-treated CXCL10⁻/⁻ mice compared to the corneas and TG of untreated CXCL10⁻/⁻ mice (Fig. 6F and G; $P > 0.05$).

The IFN-γ production by CD8⁺ T cells within both the cornea and TG of CXCL10⁻/⁻ deficient mice treated with rAAV8-CXCL10 was improved to a significantly higher level compared to untreated CXCL10⁻/⁻ deficient mice ($P = 0.05$; Fig. 7A and B). The
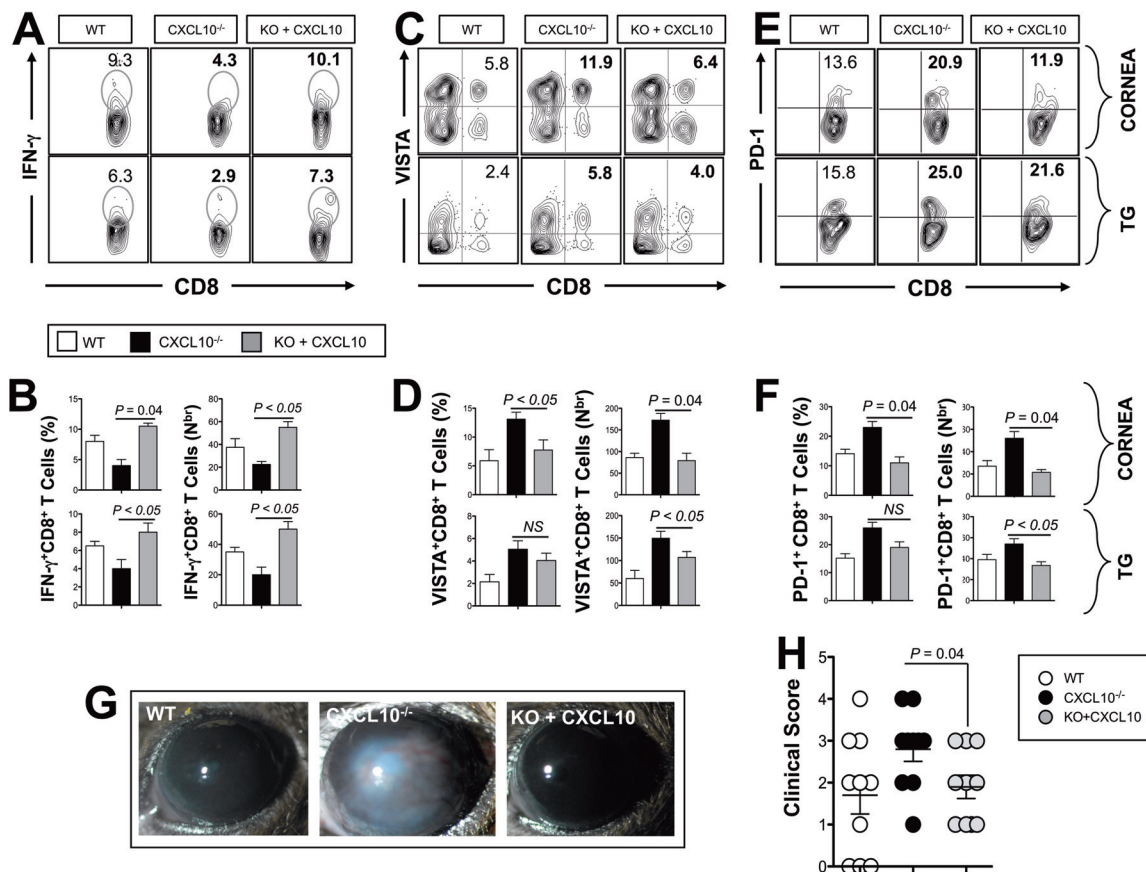
FIG 7 Topical ocular application of neurotropic AAV8 vector expressing CXCL10 promotes the function of antiviral CD8+ T cells in the trigeminal ganglia and corneas of CXCL10−/− mice. WT B6 and CXCL10−/− mice were ocularly infected using 2×10^5 wild-type McKrae (HSV-1) strain. At 24 days postinfection, when latency was fully established, reactivation of latent HSV-1 infection was induced after UV-B irradiation. Six days after UV-B irradiation, the CXCL10−/− mice were treated with rAAV8-CXCL10 using 1×10^7 PFU in each eye. Single-cell suspensions from corneas and TG were obtained after collagenase treatment at 37°C for an hour and stained for CD8+ T cells, IFN-γ, VISTA, and PD-1 and analyzed by FACS. (A, C, and E) Representative FACS plots of the frequencies of HSV-specific IFN-γ+ CD8+ T cells (A), VISTA+ CD8+ T cells (C), and PD-1+ CD8+ T cells (E) detected in the corneas and TG of WT and CXCL10−/− mice untreated and treated with rAAV8-CXCL10. (B, D, and F) Average percentages (left) and absolute numbers (right) of HSV-specific IFN-γ+ CD8+ T cells (B), VISTA+ CD8+ T cells (D), and PD-1+ CD8+ T cells (F) detected in the corneas and TG of WT and CXCL10−/− mice untreated and treated with rAAV8-CXCL10. (G and H) Recurrent corneal herpetic disease was monitored for up to 30 days after UV-B irradiation and rAAV8-CXCL10 treatment. CXCL10−/− mice were observed daily for eye disease and clinically scored on a scale of 0 to 4. The results are representative of two independent experiments. The indicated P values, calculated using unpaired t test, show statistical significance between WT and CXCL10−/− deficient mice.

exhaustion of cornea- and TG-resident CD8+ T cells appeared to be reversed following CXCL10 local treatment, as fewer VISTA+ CD8+ T cells (Fig. 7C and D) and fewer PD-1+ CD8+ T cells (Fig. 7E and F) were detected in TG and corneas of CXCL10−/− mice following treatment with rAAV8-CXCL10 compared to untreated mice. Finally, significantly less severe (Fig. 7G) and less frequent (Fig. 7H) recurrent corneal herpetic disease was detected in CXCL10−/− deficient mice that were treated with rAAV8-CXCL10 compared to untreated CXCL10−/− mice. In contrast, no effect on corneal herpetic disease was seen in CXCL10−/− mice treated with rAAV8-CXCL9 or an empty rAAV8 vector (data not shown).

Altogether, these results demonstrate for the first time a successful coexpression of the neurotropic recombinant adeno-associated virus type 8 bearing GFP and CXCL10 chemokine in latently infected trigeminal ganglia of CXCL10−/− mice following topical ocular application. These results also demonstrate for the first time that topical ocular application of neurotropic rAAV8 vector expressing CXCL10 chemokine increased the number of CD8+ T_{EM} and T_{RM} cells in latently infected TG, reversed their dysfunction, and rescued their protective function against recurrent herpetic disease following reactivation.

DISCUSSION

In the present study, we demonstrate that the lack of CXCL10 chemokine or its receptor CXCR3 compromises the mobilization of functional CD8$^+$ T$_{EM}$ and CD8$^+$ T$_{RM}$ cells within TG of latently infected mice following UV-B-induced reactivation. This is associated with an increase in recurrent ocular herpesvirus infection and disease. Inversely, increasing the amount of CXCL10 in TG of latently infected CXCL10-deficient mice rescued local CD8$^+$ T$_{EM}$ and CD8$^+$ T$_{RM}$ cell responses and improved protection against recurrent ocular herpes. Based on these findings, a novel "prime/pull" therapeutic ocular herpes vaccine strategy that would increase the number of functional CD8$^+$ T$_{EM}$ and CD8$^+$ T$_{RM}$ cells within HSV-1 latently infected TG is proposed and discussed.

Work from our laboratory and others has shown that the CD8$^+$ T cells are critical for protection against recurrent ocular herpesvirus infection and disease (23, 24, 39). However, the relative contribution of each of the CD8$^+$ T cell subpopulations in protection against recurrent herpes has not been reported. The three major subpopulations of memory T cells (i.e., CD8$^+$ T$_{EM}$ cells, CD8$^+$ T$_{CM}$ cells, and CD8$^+$ T$_{RM}$ cells) differ in their phenotype, function, and anatomic distribution (12, 14, 40). T$_{CM}$ cells are CD103^{low} CD62L^{high} CCR7^{high}. T$_{EM}$ cells are CD103^{low} CD62L^{low} CCR7^{low}. T$_{RM}$ cells are CD103^{high} CD62L^{low} CCR7^{low} CD11a^{high} CD69^{high} (12, 14, 40). Compared to T$_{CM}$ cells which reside mostly in lymphoid tissues, T$_{EM}$ cells, which reside mostly in nonlymphoid tissues, have a decreased ability to traffic to lymphoid tissues and lack CD62L and CCR7 (molecules directing lymph node entry) and express chemokine receptors such as CCR5 that are associated with homing to inflammatory sites (41, 42). Compared to T$_{CM}$ and T$_{EM}$ cells, the T$_{RM}$ cells are generated locally within peripheral tissues, do not reenter the circulation system, and appear therefore to play an essential role in locally guarding these peripheral tissues from secondary infections. To the best of our knowledge, this is the first report that demonstrates a crucial role for both the CD8$^+$ T$_{EM}$ and CD8$^+$ T$_{RM}$ cell subpopulations, but not the CD8$^+$ T$_{CM}$ subpopulation, in protection against recurrent herpesvirus infection and disease. Thus, based on these new findings, a worthy goal of a herpes immunotherapeutic vaccine should be to develop a vaccine strategy that would generate and maintain a sufficient number of antiviral memory CD8$^+$ T$_{EM}$ and CD8$^+$ T$_{RM}$ cells within peripheral tissues, such as latently infected TG, the root of virus reactivation that leads to virus shedding and recurrent ocular herpetic disease (23–26). However, this goal remains unattainable because the TG appear to be a "closed immunological compartment" to accepting homing of conventional circulating memory CD8$^+$ T cell subpopulations such as the CD8$^+$ T$_{EM}$ cells that could be migrating into latently infected TG from the neighboring draining lymph nodes through the circulation system (14, 43). To overcome this challenge, our study demonstrates for the first time that changing the microenvironment of latently infected TG in CXCL10$^{-/-}$ deficient mice by increasing the amount of local CXCL10 chemokine had the following effects: (i) rescued the number of both CD8$^+$ T$_{EM}$ and CD8$^+$ T$_{RM}$ cell subpopulations in TG, (ii) reversed the exhaustion of CD8$^+$ T$_{EM}$ and CD8$^+$ T$_{RM}$ cells in TG, and (iii) reduced recurrent corneal herpetic disease. It is likely that accumulation of a sufficient number of CD8$^+$ T$_{EM}$ and CD8$^+$ T$_{RM}$ cells within latently infected TG, by a yet-to-be determined CXCL10/CXCR3-dependent mechanism, reduced virus reactivation from latency. Since the TG appear to be an immunological compartment that is closed during latency to accepting homing of circulating CD8$^+$ T$_{CM}$ and CD8$^+$ T$_{EM}$ cells, which could be coming from the draining lymph nodes through the circulation system (14, 43), it is very likely that T$_{RM}$ cells are the main T cell subpopulation that contribute to suppressing (or aborting) attempts of HSV-1 reactivation from latently infected neurons.

An average percentage of 7.5% to 12.5% of CXCR3$^+$ CD8$^+$ T cells was detected in latently infected wild-type mice compared to an average low percentage of 2 to 2.5% CXCR3$^+$ CD8$^+$ T cells in latently infected CXCR3$^{-/-}$ and CXCL10$^{-/-}$ mice. An immediate practical application of these findings is the development of an ocular herpes

"prime/prime" immunotherapeutic vaccine strategy that will include T cell-attracting chemokines, such as the CXCL10 chemokine, to "pull" more antiviral CD8+ T cells from the circulation system and boost their number and function within latently infected TG. A powerful "prime/pool" immunotherapeutic vaccine might be expected to stop or reduce reactivation of HSV-1 from latency with the potential to produce a sustained clinical reduction of blinding recurrent herpetic disease. A human "prime/pool" thera-peutic strategy is currently being explored in our laboratory using the "humanized" HLA Tg mouse and HLA Tg rabbit models of herpes reactivation. In these models, CD8+ T cells are first primed with human immunodominant CD8+ T cell epitopes selected in HSV-1 proteins (prime) and then treated with the AAV8 or AAV9 vectors expressing T cell-attracting chemokines, CXCL9, CXCL10 and CXCL11, in the TG (pull) to maintain an increase in the number of functional antiviral CD8+ T cells in TG that will reduce virus reactivation and protect against recurrent ocular herpesvirus infection and disease. This strategy is adapted from the recently reported "prime/pull" genital herpes vaccine strategy from the 2012 study of Shin and Iwasaki that used a mouse model of genital herpes (44). That study (44) first induced HSV-specific activated CD8+ T cells in the periphery (prime) and then pulled them into the vaginal mucocutaneous tissue follow-ing intravaginal administration of the CXCL10 chemokine.

Mice have been the small-animal model of choice for herpes immunologists and virologists (reviewed in reference 45). Results from many mouse models of herpesvirus infection and immunity have yielded tremendous insights into the protective and immunopathological mechanisms during primary acute infection (46–52). However, the extrapolation of results from mouse primary herpetic disease to human recurrent herpetic diseases, such as recurrent herpetic stromal keratitis (rHSK), is yet to be proven. This is mainly because the immune mechanisms that operate during primary acute infection appear to be different from those that operate during recurrent ocular herpetic diseases (53–55). Thus, the inadequacy of many currently used mouse models of primary acute herpesvirus infection makes it challenging to explore the immune mechanisms that lead to protection against recurrent herpes (56). A critical question remains as to which animal model would be the most appropriate to mimic the immunoprotective versus immunopathological aspect of recurrent herpes as occurs in humans? Unlike humans, spontaneous HSV-1 reactivation in latently infected mice and virus shedding in tears either does not occur at all or occurs at very low levels in mice (57). Only a handful of studies have employed the mouse model of UV-B light-induced recurrent herpetic corneal disease, mostly using C57BL/6 and BALB/c mice (54, 55, 58). The present study validated the UV-B light-induced recurrent herpetic corneal disease in the "humanized" HLA transgenic mouse model of ocular herpes (4, 24). The study demonstrated that both shedding of reactivated virus in tears and recurrent corneal HSV can be induced following UV-B exposure of latently infected HLA Tg mice. Moreover, considering the wealth of data addressing the protective mechanisms of CD8+ T cells specific to mouse HSV-1 epitopes (mostly the $gB_{498-505}$ epitope in B6 mice), it is surprising how few reports exist exploring the protective mechanisms of CD8+ T cells specific to human HSV-1 epitopes (27, 54, 58, 59). Our "humanized" HLA Tg mice express the human HLA-A*0201 molecule, instead of mouse H2^b major histocompatibility complex (MHC) molecules (4). Using the UV-B/HLA Tg mouse model of recurrent ocular herpes, it is now possible to directly evaluate the efficacy of therapeutic herpes vaccine candidates that include human HLA-restricted CD8+ T cell epitopes. In our opinion, the HLA Tg mice combined with UV-B-induced recurrent disease is arguably the best available small-animal model to study the role of HLA-restricted CD8+ T cells specific to human HSV-1 epitopes in protection against virus shedding and recurrent herpetic disease.

The cellular and molecular mechanisms by which the CXCL10/CXCR3 chemokine axis (i) regulates trafficking and mobilization of HSV-specific CD8+ T_{EM} and CD8+ T_{RM} cells into HSV-1 latently infected TG and (ii) orchestrates CD8+ T cell-mediated protec-tive immunity to virus reactivation and subsequent recurrent herpetic disease remain to be determined. Wuest and Carr have previously demonstrated that, following

corneal HSV-1 infection, both CXCL10 and CXCR3 played a role in reducing primary infection in the nervous system (31). The authors suggested that recruitment of CXCL10-expressing hematopoietic cells, dendritic cells, NK cells, and HSV-specific CD8+ T cells to the brain stem plays a role in controlling viral replication in the nervous system (60). CXCL10 deficiency was associated with a reduction in the mobilization of HSV-specific CD8+ T cells into the brain as a result of dysregulation of CXCR3 signaling (31). CXCR3$^{-/-}$ deficient mice are also reported to be susceptible to primary genital HSV-2 infection (61–64). This susceptibility appeared to be associated with reduced cytotoxic function of CD8+ T cells through impairment in expression of T-bet, perforin, and GzmB, as well as a reduction in the recruitment of pDC and impairment in CD80 expression on CD11c+ DC (61–64). It is important to underline that, unlike the above studies that were done using mouse models of acute ocular and genital primary infections, our present studies used a mouse model of induced virus reactivation and recurrent herpes. Since the immune mechanisms that operate during primary acute and recurrent herpes infections are often different, the extrapolation of the above findings in primary/acute infection to our latency/reactivation model remains to be seen (53–55). Moreover, the above studies that used mouse models of ocular and genital primary infections did not report whether generation and mobilization of memory T_{CM}, T_{EM}, and T_{RM} cell subpopulations were affected beyond the acute phase of infection.

It is likely that CXCL10, which is produced locally by neurons, macrophages, epithelial cells, and T cells among other cells (14, 43), contributes to the accumulation and function of CXCR3+ CD8+ T_{EM} and CXCR3+ CD8+ T_{RM} cells in the TG and cornea. Moreover, an elevated amount of IFN-γ produced by CD8+ T cells may also contribute to the generation of even more functional CXCR3+ CD8+ T_{EM} and CXCR3+ CD8+ T_{RM} cells in TG and corneal tissues. Compared to WT B6 mice, CXCL10$^{-/-}$ deficient mice developed significantly less functional CXCR3+ CD8+ T_{EM} and CXCR3+ CD8+ T_{RM} cells in both TG and cornea and failed to contain recurrent ocular herpesvirus infection and disease. Furthermore, a significant reduction in the IFN-γ production by TG and cornea-resident CD8+ T cells was observed in CXCL10$^{-/-}$ deficient mice. Increased numbers of exhausted CD8+ T cells, expressing high levels of PD-1, V-domain Ig suppressor of T cell activation (VISTA), and T cell Ig and ITIM domain (TIGIT) (VISTA and TIGIT recently discovered markers of exhaustion), were detected in TG and corneas of CXCL10$^{-/-}$ deficient mice and were associated with the failure to contain recurrent ocular herpes. This suggests that the CXCL10/CXCR3 chemokine signaling pathway contributes, with a yet-to-be determined mechanism, to the generation of a large repertoire of exhausted HSV-specific CD8+ T cells within latently infected TG, similar to the finding we recently reported in HLA Tg rabbits (16). The finding that TG-resident CD8+ T cells recognized HSV-1 human epitopes and expressed high levels of PD-1, TIGIT, and VISTA differs from a recent suggestion that these cells are fully functional (65).

The current largely accepted paradigm is that exhaustion of T cells requires persistent exposure to a large amount of antigen (Ag). The amount of viral Ag produced in the latently infected TG of mice following UV-B reactivation is quite low, less than 1 positive neuron/TG (66–69). Thus, it is likely that the CXCL10/CXCR3 chemokine pathway inhibits exhaustion of CD8+ T cells in TG through mechanisms other than Ag persistence, as we previously discussed (70). Elucidating the mechanisms by which the CXCL10/CXCR3 pathway might be preventing CD8+ T cell exhaustion is beyond the scope of the present study. Nevertheless, our results demonstrate, for the first time, that the CXCL10/CXCR3 chemokine signaling pathway is of paramount importance in T cell immunity against recurrent ocular herpes. The results also suggest that coblockade of the PD-1, VISTA, and TIGIT immune checkpoints should be further explored to elicit potent antiviral CXCR3+ CD8+ T_{EM} and CXCR3+ CD8+ T_{RM} cell responses that could control or eliminate recurrent ocular herpes.

A high level of expression of PD-1 alone on T cells does not necessarily prove functional exhaustion. Both activated and exhausted T cells express PD-1, with ex-

hausted T cells expressing higher and more persistent levels of PD-1 than activated T cells do (68, 71, 72). Therefore, instead of relying only on the level of expression of PD-1, in the present study, we also determined coexpression of TIM-3 and 2B4 markers of exhaustion on CD8+ T cells, as well as of two newly reported markers of exhaustion, TIGIT and VISTA (36–38, 73). PD-1, TIM-3, 2B4, TGIT, and VISTA were all coexpressed at various levels on CD8+ T cells from TG of CXCL10$^{-/-}$ deficient mice compared to CD8+ T cells from TG of age- and sex-matched WT B6 mice. Mobilization of PD-1+ CD8+ T cells, TIM3+ CD8+ T cells, 2B4+ CD8+ T cells, TGIT+ CD8+ T cells, and VISTA+ CD8+ T cells in TG of CXCL10$^{-/-}$ deficient mice point to exhausted (dysfunctional) CD8+ T cells in TG. This was confirmed at the functional level by a decrease in the levels of CD107$^{a/b}$ cytotoxic degranulation and by lower production of both IFN-γ and tumor necrosis factor alpha (TNF-α). These results are consistent with our recent finding of a significantly higher level of exhaustion of HSV-1 human epitope-specific CD8+ T cells from TG of HLA Tg rabbits with higher virus reactivation compared to TG of HLA Tg rabbits with less virus reactivation (1, 7, 74). Because HSV-1 might coopt PD-1, TIM-3, 2B4, VISTA and/or TIGIT immune checkpoints as a strategy to evade CD8+ T cell immune surveillance (70, 75), a T cell-based immunotherapy will likely have to be combined with immune checkpoint blockade in order to reverse the dysfunction of antiviral CD8+ T$_{EM}$ and CD8+ T$_{RM}$ cells. Antibodies targeting the PD-1/PD-L1 (programmed death ligand 1) immune checkpoint have recently shown remarkable clinical safety and efficacy in other systems (76–78). The current largely accepted paradigm is that exhaustion of T cells requires persistent exposure to Ag (66–69). Elucidating the mechanisms by which the CXCL10/CXCR3 pathway might be preventing CD8+ T cell exhaustion remains to be determined. It is likely that the CXCL10/CXCR3 chemokine pathway prevents exhaustion of CD8+ T cells through mechanisms other than Ag persistence (70).

In conclusion, this study represents the first in-depth analysis of the role of the CXCL10/CXCR3 axis in the mobilization of HSV-specific CD8+ T$_{EM}$, T$_{CM}$, and T$_{RM}$ cell subpopulations in latently infected trigeminal ganglia and corneas. We demonstrate that, following UV-B-induced recurrent ocular herpes, mobilization of functional IFN-γ-producing cytotoxic CXCR3+ CD8+ T$_{EM}$ and CXCR3+ CD8+ T$_{RM}$ cells into TG was associated with protection against recurrent herpes. In contrast, phenotypically and functionally exhausted CD8+ T$_{EM}$ and CD8+ T$_{RM}$ cells were associated with the failure to contain recurrent ocular herpesvirus infection and disease. Based on these findings, this study proposes and discusses a novel "prime/pull" immunotherapeutic herpes vaccine approach, which would employ human CD8+ T cell epitopes together with delivery of T cell-attracting chemokines, such as CXCL10, within latently infected TG, using safe neurotropic vectors, such as AAV8, in combination with an immune checkpoint blockade.

MATERIALS AND METHODS

Mice. CXCR3- and CXCL10-deficient mice (CXCR3$^{-/-}$ and CXCL10$^{-/-}$ mice) (6 to 8 weeks old; on the C57BL/6 background) and female C57BL/6 (B6) wild-type (WT) mice (6 to 8 weeks old) were purchased from Jackson Laboratory (Bar Harbor, ME). Animal studies were performed conforming to the *Guide for the Care and Use of Laboratory Animals* (79). Experiments were conducted with the approval of the Institutional Care and Use Committee of University of California Irvine (Irvine, CA).

Ocular infection with HSV-1. HSV-1 (strain McKrae) was grown and titrated on rabbit skin (RS) cells. Mice were infected with 2×10^5 PFU of strain McKrae via eye drops. Following ocular infection, mice were monitored for ocular herpesvirus infection and disease.

UV-B irradiation of latently infected mouse eyes and monitoring recurrent eye disease. Reactivation of latent HSV-1 was induced in latently infected mice following UV-B irradiation as we recently described (5, 6). Briefly, 24 days postinfection, when latency was fully established, anesthetized mice were placed on the transilluminator, and each mouse was positioned on a piece of cardboard containing a hole the same size as the mouse's eye, allowing a single eye to be irradiated by the UV-B source. Each eye was then irradiated with 250 mJ of UV-B light cm² (60-s exposure on the transilluminator). On days 1 to 6 after UV-B irradiation, eyes were swabbed using a Dacron swab, and samples were frozen at −80°C for viral titer analysis. Animals were examined for signs of recurrent corneal herpetic disease by using a slit lamp for 30 days after UV-B irradiation. Animal examinations were performed by investigators blind to the treatment regimen of the mice as previously described (55). The severity of recurrent disease was scored according to a standard scale scored from 0 to 4 (0 for no disease, 1 for 25% disease, 2 for 50% disease, 3 for 75% disease, and 4 for 100% disease) as previously described (2, 80, 81).

Viral titer assay. Eye swabs (tears) were analyzed for viral titers by plaque assays. Vero cells were grown in α-modified Eagle's medium (Thermo Scientific, Waltham, MA) supplemented with 5% fetal bovine serum and 1% penicillin-streptomycin, and L-glutamine (Thermo Scientific). For plaque assays, Vero cells were grown to 70% confluence in 24-well plates. Tear samples were diluted and then added to monolayers. Infected monolayers were incubated at 37°C for 1 h and were rocked every 15 min for viral absorption. Infected monolayers were overlaid with an overlay medium containing carboxymethyl cellulose. Infection was allowed to occur for 72 h at 37°C. Monolayers were then fixed and stained with crystal violet, and viral plaques were counted under a light microscope. Positive controls were run with every assay using previously titered laboratory stocks of HSV-1 (strain McKrae).

Design and construction of AAV8 vector expressing mouse CXCL9 or CXCL10 chemokine under a calcium/calmodulin-dependent protein kinase type II subunit alpha (CamKII-α) neurotropic promoter. The open reading frame (ORF) for mouse CXCL9 or CXCL10 was cloned into SalI/EcoRI sites of pAAV-CamKII-MCS-CamKII-EGFP (MCS stands for multiple cloning site, and EGFP stands for enhanced GFP) vector. This pAAV vector was cotransfected with helper plasmid in HEK293 cells to produce the AAV virus. Two days after transfections, cell pellets were harvested, and viruses were released through three cycles of freeze-thawing. AAV viruses were purified through CsCl gradient ultracentrifugation, followed by desalting. Viral titers (in genome copies [GC] per milliliter) were determined through real-time PCR.

Topical administration of neurotropic AAV8 vector expressing mouse CXCL9 or CXCL10 chemokine under a CamKII neurotropic promoter. On day 6 after UV-B irradiation, a group of CXCL10$^{-/-}$ mice were anesthetized and corneas were scarified (i.e., the epithelium was lightly scratched) in a crosshatched pattern of four to five vertical scratches and four to five horizontal scratches using a 25-gauge needle. Mice were then treated topically with AAV8-CamKIIa-mCXCL10-CamKIIa-eGFP using 1×10^7 PFU in each eye. Mice were euthanized at day 2 after AAV8-CamKIIa-mCXCL10-CamKIIa-eGFP treatments.

Isolation of single-cell and flow cytometry. Mice from all three groups (CXCR3$^{-/-}$, CXCL10$^{-/-}$, and B6) were euthanized and the draining lymph node (DLN), cornea, and trigeminal ganglia (TG) were individually harvested. Tissues were digested in complete medium containing 2.5 mg/ml collagenase type IV (Sigma Chemical Co., St. Louis, MO). Digestion was accomplished by incubation at 37°C with shaking for 30 min. After digestion, tissues and cells were filtered through a sterile gauze mesh and washed with RPMI 1640 medium. Single-cell suspensions were prepared and analyzed using flow cytometry.

The following antibodies were used: peridinin chlorophyll protein (PerCP)-labeled anti-mouse CD8 (clone 53-6.7; BD Biosciences, San Jose, CA), fluorescein isothiocyanate (FITC)-labeled anti-mouse CD11a (clone M17/4; BD), allophycocyanin (APC)-labeled anti-mouse CD103 (clone M290; BD), anti-mouse CD62L A700 (clone MEL-14; BD Biosciences), APC-Cy7-labeled anti-mouse CD44 (clone IM7; BioLegend, San Diego, CA), phycoerythrin (PE)-Cy7-labeled anti-mouse CD69 (clone H1.2F3; BD), anti-mouse CCR7 A647 (clone 4B12; BD), PE-labeled TIGIT (clone GIGD7; Ebiosciences), VISTA (clone 13f3; a gift from R. J. Noelle, Geisel School of Medicine at Dartmouth, Lebanon, NH), APC-labeled anti-mouse PD-1 (clone J43; BD), FITC-labeled anti-mouse 2B4 (clone m2B4; Biolegend), PE-Cy7-labeled Tim-3 (BD), PE-labeled anti-mouse IFN-γ (clone XMG1.2; BioLegend), and PE-Cy7-labeled anti-mouse TNF-α (BioLegend). For surface staining, MAbs against various cell markers were added to a total of 1×10^6 cells in phosphate-buffered saline (PBS) containing 1% fetal bovine serum (FBS) and 0.1% sodium azide (fluorescence-activated cell sorting [FACS] buffer) and left for 45 min at 4°C. For intracellular staining, cells were first treated with Cytofix/Cytoperm (BD Biosciences) for 30 min. After washing with Perm/Wash buffer, monoclonal antibodies (MAbs) were added to the cells and incubated for 45 min on ice in the dark. The cells were washed again with Perm/Wash and FACS buffer and fixed in PBS containing 2% paraformaldehyde (Sigma-Aldrich). To define tissue-resident memory CD8$^+$ T cells (T$_{RM}$), live lymphocytes were gated based on their forward and side scatter properties. The CD8-positive cells were then further identified and gated. To identify tissue-resident memory CD8$^+$ T cells (CD8$^+$ T$_{RM}$ cells), a sequential gating of CCR7^{low} CD11a^{high} CD69^{high} was performed on the CD8-positive cells.

For the measurement of TNF-α and IFN-γ, 1×10^6 cells were transferred into a 96-well flat-bottom plate in the presence of BD GolgiStop (10 μg/ml) for 6 h at 37°C. Phytohemagglutinin (PHA) (5 μg/ml) (Sigma-Aldrich) was used as a positive control. At the end of the incubation period, the cells were transferred to a 96-well round-bottom plate and washed once with FACS buffer. Surface and intracellular staining were performed as described above. A total of 100,000 events were acquired by LSRII (Becton Dickinson, Mountain View, CA) followed by analysis using FlowJo software (TreeStar, Ashland, OR).

Statistical analysis. Data for each assay were compared by analysis of variance (ANOVA) and unpaired t test using Graph Pad Prism 5 software (San Diego, CA). Differences between the groups were identified using unpaired t test, multiple comparison Mann-Whitney test and two-tail analyses, as we previously described (23). Data are expressed as means ± standard deviations (SD). Results were considered to be statistically significant at a P value of <0.05.

SUPPLEMENTAL MATERIAL

Supplemental material for this article may be found at https://doi.org/10.1128/JVI .00278-17.

SUPPLEMENTAL FILE 1, PDF file, 0.4 MB.

REFERENCES

1. Srivastava R, Khan AA, Spencer D, Vahed H, Lopes PP, Thai NT, Wang C, Pham TT, Huang J, Scarfone VM, Nesburn AB, Wechsler SL, BenMohamed L. 2015. HLA-A02:01-restricted epitopes identified from the herpes simplex virus tegument protein VP11/12 preferentially recall polyfunctional effector memory CD8+ T cells from seropositive asymptomatic individuals and protect humanized HLA-A*02:01 transgenic mice against ocular herpes. J Immunol 194:2232–2248. https://doi.org/10.4049/jimmunol.1402606.

2. Samandary S, Kridane-Miledi H, Sandoval JS, Choudhury Z, Langa-Vives F, Spencer D, Chentoufi AA, Lemonnier FA, BenMohamed L. 2014. Associations of HLA-A, HLA-B and HLA-C alleles frequency with prevalence of herpes simplex virus infections and diseases across global populations: implication for the development of an universal CD8+ T-cell epitope-based vaccine. Hum Immunol 75:715–729. https://doi.org/10.1016/j.humimm.2014.04.016.

3. Looker KJ, Magaret AS, May MT, Turner KM, Vickerman P, Gottlieb SL, Newman LM. 2015. Global and regional estimates of prevalent and incident herpes simplex virus type 1 infections in 2012. PLoS One 10:e0140765. https://doi.org/10.1371/journal.pone.0140765.

4. Dervillez X, Qureshi H, Chentoufi AA, Khan AA, Kritzer E, Yu DC, Diaz OR, Gottimukkala C, Kalantari M, Villacres MC, Scarfone VM, McKinney DM, Sidney J, Sette A, Nesburn AB, Wechsler SL, BenMohamed L. 2013. Asymptomatic HLA-A*02:01-restricted epitopes from herpes simplex virus glycoprotein B preferentially recall polyfunctional CD8+ T cells from seropositive asymptomatic individuals and protect HLA transgenic mice against ocular herpes. J Immunol 191:5124–5138. https://doi.org/10.4049/jimmunol.1301415.

5. BenMohamed L, Osorio N, Srivastava R, Khan AA, Simpson JL, Wechsler SL. 2015. Decreased reactivation of a herpes simplex virus type 1 (HSV-1) latency-associated transcript (LAT) mutant using the in vivo mouse UV-B model of induced reactivation. J Neurovirol 21:508–517. https://doi.org/10.1007/s13365-015-0348-9.

6. BenMohamed L, Osorio N, Khan AA, Srivastava R, Huang L, Krochma JJ, Garcia LM, Simpson JL, Wechsler SL. 2016. Prior corneal scarification and injection of immune serum are not required before ocular HSV-1 infection for UV-B-induced virus reactivation and recurrent herpetic corneal disease in latently infected mice. Curr Eye Res 41:747–756. https://doi.org/10.3109/02713683.2015.1061024.

7. Khan AA, Srivastava R, Chentoufi AA, Geertsema R, Thai NT, Dasgupta G, Osorio N, Kalantari M, Nesburn AB, Wechsler SL, BenMohamed L. 2015. Therapeutic immunization with a mixture of herpes simplex virus 1 glycoprotein D-derived "asymptomatic" human CD8+ T-cell epitopes decreases spontaneous ocular shedding in latently infected HLA transgenic rabbits: association with low frequency of local PD-1+ TIM-3+ CD8+ exhausted T cells. J Virol 89:6619–6632. https://doi.org/10.1128/JVI.00788-15.

8. Farooq AV, Shukla D. 2012. Herpes simplex epithelial and stromal keratitis: an epidemiologic update. Surv Ophthalmol 57:448–462. https://doi.org/10.1016/j.survophthal.2012.01.005.

9. Herpetic Eye Disease Study Group. 1998. Acyclovir for the prevention of recurrent herpes simplex virus eye disease. N Engl J Med 339:300–306. https://doi.org/10.1056/NEJM199807303390503.

10. Kuo T, Wang C, Badakhshan T, Chilukuri S, BenMohamed L. 2014. The challenges and opportunities for the development of a T-cell epitope-based herpes simplex vaccine. Vaccine 32:6733–6745. https://doi.org/10.1016/j.vaccine.2014.10.002.

11. Mackay LK, Gebhardt T. 2013. Tissue-resident memory T cells: local guards of the thymus. Eur J Immunol 43:2259–2262. https://doi.org/10.1002/eji.201343930.

12. Gebhardt T, Mackay LK. 2012. Local immunity by tissue-resident CD8+ memory T cells. Front Immunol 3:340. https://doi.org/10.3389/fimmu.2012.00340.

13. Ariotti S, Beltman JB, Chodaczek G, Hoekstra ME, van Beek AE, Gomez-Eerland R, Ritsma L, van Rheenen J, Maree AF, Zal T, de Boer RJ, Haanen JB, Schumacher TN. 2012. Tissue-resident memory CD8+ T cells continuously patrol skin epithelia to quickly recognize local antigen. Proc Natl Acad Sci U S A 109:19739–19744. https://doi.org/10.1073/pnas.1208927109.

14. Gebhardt T, Whitney PG, Zaid A, Mackay LK, Brooks AG, Heath WR, Carbone FR, Mueller SN. 2011. Different patterns of peripheral migration by memory CD4+ and CD8+ T cells. Nature 477:216–219. https://doi.org/10.1038/nature10339.

15. Srivastava R, Khan AA, Huang J, Nesburn AB, Wechsler SL, BenMohamed L. 2015. A herpes simplex virus type 1 human asymptomatic CD8+ T-cell epitopes-based vaccine protects against ocular herpes in a "humanized" HLA transgenic rabbit model. Invest Ophthalmol Vis Sci 56:4013–4028. https://doi.org/10.1167/iovs.15-17074.

16. Srivastava R, Dervillez X, Khan AA, Chentoufi AA, Chilukuri S, Shukr N, Fazli Y, Ong NN, Afifi ER, Osorio N, Geertsema R, Nesburn AB, Wechsler SL, BenMohamed L. 2016. The herpes simplex virus latency-associated transcript gene is associated with a broader repertoire of virus-specific exhausted CD8+ T cells retained within the trigeminal ganglia of latently infected HLA transgenic rabbits. J Virol 90:3913–3928. https://doi.org/10.1128/JVI.02450-15.

17. Arbusow V, Derfuss T, Held K, Himmelein S, Strupp M, Gurkov R, Brandt T, Theil D. 2010. Latency of herpes simplex virus type-1 in human geniculate and vestibular ganglia is associated with infiltration of CD8+ T cells. J Med Virol 82:1917–1920. https://doi.org/10.1002/jmv.21904.

18. Derfuss T, Arbusow V, Strupp M, Brandt T, Theil D. 2009. The presence of lytic HSV-1 transcripts and clonally expanded T cells with a memory effector phenotype in human sensory ganglia. Ann N Y Acad Sci 1164:300–304. https://doi.org/10.1111/j.1749-6632.2009.03871.x.

19. Derfuss T, Segerer S, Herberger S, Sinicina I, Hufner K, Ebelt K, Knaus HG, Steiner I, Meinl E, Dornmair K, Arbusow V, Strupp M, Brandt T, Theil D. 2007. Presence of HSV-1 immediate early genes and clonally expanded T-cells with a memory effector phenotype in human trigeminal ganglia. Brain Pathol 17:389–398. https://doi.org/10.1111/j.1750-3639.2007.00088.x.

20. Held K, Derfuss T. 2011. Control of HSV-1 latency in human trigeminal ganglia—current overview. J Neurovirol 17:518–527. https://doi.org/10.1007/s13365-011-0063-0.

21. Held K, Eiglmeier I, Himmelein S, Sinicina I, Brandt T, Theil D, Dornmair K, Derfuss T. 2012. Clonal expansions of CD8+ T cells in latently HSV-1-

infected human trigeminal ganglia. J Neurovirol 18:62–68. https://doi
.org/10.1007/s13365-011-0067-9.

22. Held K, Junker A, Dornmair K, Meinl E, Sinicina I, Brandt T, Theil D, Derfuss T. 2011. Expression of herpes simplex virus 1-encoded micro-RNAs in human trigeminal ganglia and their relation to local T-cell infiltrates. J Virol 85:9680–9685. https://doi.org/10.1128/JVI.00874-11.

23. Zhang X, Chentoufi AA, Dasgupta G, Nesburn AB, Wu M, Zhu X, Carpenter D, Wechsler SL, You S, BenMohamed L. 2009. A genital tract peptide epitope vaccine targeting TLR-2 efficiently induces local and systemic CD8+ T cells and protects against herpes simplex virus type 2 challenge. Mucosal Immunol 2:129–143. https://doi.org/10.1038/mi.2008.81.

24. Zhang X, Dervillez X, Chentoufi AA, Badakhshan T, Bettahi I, Benmohamed L. 2012. Targeting the genital tract mucosa with a lipopeptide/recombinant adenovirus prime/boost vaccine induces potent and long-lasting CD8+ T cell immunity against herpes: importance of MyD88. J Immunol 189:4496–4509. https://doi.org/10.4049/jimmunol.1201121.

25. Steinert EM, Schenkel JM, Fraser KA, Beura LK, Manlove LS, Igyarto BZ, Southern PJ, Masopust D. 2015. Quantifying memory CD8 T cells reveals regionalization of immunosurveillance. Cell 161:737–749. https://doi
.org/10.1016/j.cell.2015.03.031.

26. Schenkel JM, Fraser KA, Masopust D. 2014. Resident memory CD8 T cells occupy frontline niches in secondary lymphoid organs. J Immunol 192:2961–2964. https://doi.org/10.4049/jimmunol.1400003.

27. Himmelein S, St Leger AJ, Knickelbein JE, Rowe A, Freeman ML, Hendricks RL. 2011. Circulating herpes simplex type 1 (HSV-1)-specific CD8+ T cells do not access HSV-1 latently infected trigeminal ganglia. Herpesviridae 2:5. https://doi.org/10.1186/2042-4280-2-5.

28. Mackay LK, Wakim L, van Vliet CJ, Jones CM, Mueller SN, Bannard O, Fearon DT, Heath WR, Carbone FR. 2012. Maintenance of T cell function in the face of chronic antigen stimulation and repeated reactivation for a latent virus infection. J Immunol 188:2173–2178. https://doi.org/10.4049/jimmunol.1102719.

29. Mackay LK, Stock AT, Ma JZ, Jones CM, Kent SJ, Mueller SN, Heath WR, Carbone FR, Gebhardt T. 2012. Long-lived epithelial immunity by tissue-resident memory T (TRM) cells in the absence of persisting local antigen presentation. Proc Natl Acad Sci U S A 109:7037–7042. https://doi.org/10.1073/pnas.1202288109.

30. Ariotti S, Beltman JB, Borsje R, Hoekstra ME, Halford WP, Haanen JB, de Boer RJ, Schumacher TN. 2015. Subtle CXCR3-dependent chemotaxis of CTLs within infected tissue allows efficient target localization. J Immunol 195:5285–5295. https://doi.org/10.4049/jimmunol.1500853.

31. Wuest TR, Carr DJ. 2008. Dysregulation of CXCR3 signaling due to CXCL10 deficiency impairs the antiviral response to herpes simplex virus 1 infection. J Immunol 181:7985–7993. https://doi.org/10.4049/jimmunol.181.11.7985.

32. Zlotnik A, Yoshie O. 2012. The chemokine superfamily revisited. Immunity 36:705–716. https://doi.org/10.1016/j.immuni.2012.05.008.

33. Zhang X, Issagholian A, Berg EA, Fishman JB, Nesburn AB, BenMohamed L. 2005. Th-cytotoxic T-lymphocyte chimeric epitopes extended by Nepsilon-palmitoyl lysines induce herpes simplex virus type 1-specific effector CD8+ Tc1 responses and protect against ocular infection. J Virol 79:15289–15301. https://doi.org/10.1128/JVI.79.24.15289-15301.2005.

34. Hickman HD, Reynoso GV, Ngudiankama BF, Cush SS, Gibbs J, Bennink JR, Yewdell JW. 2015. CXCR3 chemokine receptor enables local CD8+ T cell migration for the destruction of virus-infected cells. Immunity 42:524–537. https://doi.org/10.1016/j.immuni.2015.02.009.

35. Mahnke YD, Brodie TM, Sallusto F, Roederer M, Lugli E. 2013. The who's who of T-cell differentiation: human memory T-cell subsets. Eur J Immunol 43:2797–2809. https://doi.org/10.1002/eji.201343751.

36. Chauvin JM, Pagliano O, Fourcade J, Sun Z, Wang H, Sander C, Kirkwood JM, Chen TH, Maurer M, Korman AJ, Zarour HM. 2015. TIGIT and PD-1 impair tumor antigen-specific CD8+ T cells in melanoma patients. J Clin Invest 125:2046–2058. https://doi.org/10.1172/JCI80445.

37. Lines JL, Pantazi E, Mak J, Sempere LF, Wang L, O'Connell S, Ceeraz S, Suriawinata AA, Yan S, Ernstoff MS, Noelle R. 2014. VISTA is an immune checkpoint molecule for human T cells. Cancer Res 74:1924–1932. https://doi.org/10.1158/0008-5472.CAN-13-1504.

38. Wang L, Rubinstein R, Lines JL, Wasiuk A, Ahonen C, Guo Y, Lu LF, Gondek D, Wang Y, Fava RA, Fiser A, Almo S, Noelle RJ. 2011. VISTA, a novel mouse Ig superfamily ligand that negatively regulates T cell responses. J Exp Med 208:577–592. https://doi.org/10.1084/jem.20100619.

39. Banerjee K, Biswas PS, Rouse BT. 2005. Elucidating the protective and

40. Mackay LK, Rahimpour A, Ma JZ, Collins N, Stock AT, Hafon ML, Vega-Ramos J, Lauzurica P, Mueller SN, Stefanovic T, Tscharke DC, Heath WR, Inouye M, Carbone FR, Gebhardt T. 2013. The developmental pathway for CD103+CD8+ tissue-resident memory T cells of skin. Nat Immunol 14:1294–1301. https://doi.org/10.1038/ni.2744.

41. Sallusto F, Geginat J, Lanzavecchia A. 2004. Central memory and effector memory T cell subsets: function, generation, and maintenance. Annu Rev Immunol 22:745–763. https://doi.org/10.1146/annurev.immunol.22.012703.104702.

42. Grossman Z, Picker LJ. 2008. Pathogenic mechanisms in simian immunodeficiency virus infection. Curr Opin HIV AIDS 3:380–386. https://doi.org/10.1097/COH.0b013e3282fbaae6.

43. Mueller SN, Gebhardt T, Carbone FR, Heath WR. 2013. Memory T cell subsets, migration patterns, and tissue residence. Annu Rev Immunol 31:137–161. https://doi.org/10.1146/annurev-immunol-032712-095954.

44. Shin H, Iwasaki A. 2012. A vaccine strategy that protects against genital herpes by establishing local memory T cells. Nature 491:463–467. https://doi.org/10.1038/nature11522.

45. Dasgupta G, BenMohamed L. 2011. Of mice and not humans: how reliable are animal models for evaluation of herpes CD8+-T cell-epitopes-based immunotherapeutic vaccine candidates? Vaccine 29:5824–5836. https://doi.org/10.1016/j.vaccine.2011.06.083.

46. Wuest T, Farber J, Luster A, Carr DJ. 2006. CD4+ T cell migration into the cornea is reduced in CXCL9 deficient but not CXCL10 deficient mice following herpes simplex virus type 1 infection. Cell Immunol 243:83–89. https://doi.org/10.1016/j.cellimm.2007.01.001.

47. Conrady CD, Zheng M, Stone DU, Carr DJ. 2012. CD8+ T cells suppress viral replication in the cornea but contribute to VEGF-C-induced lymphatic vessel genesis. J Immunol 189:425–432. https://doi.org/10.4049/jimmunol.1200063.

48. Dasgupta G, Chentoufi AA, Nesburn AB, Wechsler SL, BenMohamed L. 2009. New concepts in herpes simplex virus vaccine development: notes from the battlefield. Expert Rev Vaccines 8:1023–1035. https://doi.org/10.1586/erv.09.60.

49. Chentoufi AA, Zhang X, Lamberth K, Dasgupta G, Bettahi I, Nguyen A, Wu M, Zhu X, Mohebbi A, Buus S, Wechsler SL, Nesburn AB, BenMohamed L. 2008. HLA-A*0201-restricted CD8+ cytotoxic T lymphocyte epitopes identified from herpes simplex virus glycoprotein D. J Immunol 180:426–437. https://doi.org/10.4049/jimmunol.180.1.426.

50. Chentoufi AA, Binder NR, Berka N, Durand G, Nguyen A, Bettahi I, Maillere B, BenMohamed L. 2008. Asymptomatic human CD4+ cytotoxic T-cell epitopes identified from herpes simplex virus glycoprotein B. J Virol 82:11792–11802. https://doi.org/10.1128/JVI.00692-08.

51. Knickelbein JE, Khanna KM, Yee MB, Baty CJ, Kinchington PR, Hendricks RL. 2008. Noncytotoxic lytic granule-mediated CD8+ T cell inhibition of HSV-1 reactivation from neuronal latency. Science 322:268–271. https://doi.org/10.1126/science.1164164.

52. Gaddipati S, Estrada K, Rao P, Jerome AD, Suvas S. 2015. IL-2/anti-IL-2 antibody complex treatment inhibits the development but not the progression of herpetic stromal keratitis. J Immunol 194:273–282. https://doi.org/10.4049/jimmunol.1401285.

53. West DM, Del Rosso CR, Yin XT, Stuart PM. 2014. CXCL1 but not IL-6 is required for recurrent herpetic stromal keratitis. J Immunol 192:1762–1767. https://doi.org/10.4049/jimmunol.1302957.

54. Stuart PM, Keadle TL. 2012. Recurrent herpetic stromal keratitis in mice: a model for studying human HSK. Clin Dev Immunol 2012:728480. https://doi.org/10.1155/2012/728480.

55. Morris J, Stuart PM, Rogge M, Potter C, Gupta N, Yin XT. 2012. Recurrent herpetic stromal keratitis in mice, a model for studying human HSK. J Vis Exp 2012:e4276. https://doi.org/10.3791/4276.

56. Dasgupta G, Nesburn AB, Wechsler SL, BenMohamed L. 2010. Developing an asymptomatic mucosal herpes vaccine: the present and the future. Future Microbiol 5:1–4. https://doi.org/10.2217/fmb.09.101.

57. Feldman LT, Ellison AR, Voytek CC, Yang L, Krause P, Margolis TP. 2002. Spontaneous molecular reactivation of herpes simplex virus type 1 latency in mice. Proc Natl Acad Sci U S A 99:978–983. https://doi.org/10.1073/pnas.022301899.

58. Webre JM, Hill JM, Nolan NM, Clement C, McFerrin HE, Bhattacharjee PS, Hsia V, Neumann DM, Foster TP, Lukiw WJ, Thompson HW. 2012. Rabbit and mouse models of HSV-1 latency, reactivation, and recurrent eye diseases. J Biomed Biotechnol 2012:612316. https://doi.org/10.1155/2012/612316.

59. St Leger AJ, Hendricks RL. 2011. CD8+ T cells patrol HSV-1-infected trigeminal ganglia and prevent viral reactivation. J Neurovirol 17: 528–534. https://doi.org/10.1007/s13365-011-0062-1.

60. Wuest TR, Thapa M, Zheng M, Carr DJ. 2011. CXCL10 expressing hematopoietic-derived cells are requisite in defense against HSV-1 infection in the nervous system of CXCL10 deficient mice. J Neuroimmunol 234:103–108. https://doi.org/10.1016/j.jneuroim.2011.03.006.

61. Thapa M, Carr DJ. 2008. Chemokines and chemokine receptors critical to host resistance following genital herpes simplex virus type 2 (HSV-2) infection. Open Immunol J 1:33–41. https://doi.org/10.2174/1874226200801010033.

62. Thapa M, Carr DJ. 2008. Herpes simplex virus type 2-induced mortality following genital infection is blocked by anti-tumor necrosis factor alpha antibody in CXCL10-deficient mice. J Virol 82:10295–10301. https://doi.org/10.1128/JVI.00931-08.

63. Thapa M, Welner RS, Pelayo R, Carr DJ. 2008. CXCL9 and CXCL10 expression are critical for control of genital herpes simplex virus type 2 infection through mobilization of HSV-specific CTL and NK cells to the nervous system. J Immunol 180:1098–1106. https://doi.org/10.4049/jimmunol.180.2.1098.

64. Thapa M, Carr DJ. 2009. CXCR3 deficiency increases susceptibility to genital herpes simplex virus type 2 infection: uncoupling of CD8+ T-cell effector function but not migration. J Virol 83:9486–9501. https://doi.org/10.1128/JVI.00854-09.

65. van Velzen M, Jing L, Osterhaus AD, Sette A, Koelle DM, Verjans GM. 2013. Local CD4 and CD8 T-cell reactivity to HSV-1 antigens documents broad viral protein expression and immune competence in latently infected human trigeminal ganglia. PLoS Pathog 9:e1003547. https://doi.org/10.1371/journal.ppat.1003547.

66. Day CL, Kaufmann DE, Kiepiela P, Brown JA, Moodley ES, Reddy S, Mackey EW, Miller JD, Leslie AJ, DePierres C, Mncube Z, Duraiswamy J, Zhu B, Eichbaum Q, Altfeld M, Wherry EJ, Coovadia HM, Goulder PJ, Klenerman P, Ahmed R, Freeman GJ, Walker BD. 2006. PD-1 expression on HIV-specific T cells is associated with T-cell exhaustion and disease progression. Nature 443:350–354. https://doi.org/10.1038/nature05115.

67. Vali B, Jones RB, Sakhdari A, Sheth PM, Clayton K, Yue FY, Gyenes G, Wong D, Klein MB, Saeed S, Benko E, Kovacs C, Kaul R, Ostrowski MA. 2010. HCV-specific T cells in HCV/HIV co-infection show elevated frequencies of dual Tim-3/PD-1 expression that correlate with liver disease progression. Eur J Immunol 40:2493–2505. https://doi.org/10.1002/eji.201040340.

68. Blackburn SD, Shin H, Haining WN, Zou T, Workman CJ, Polley A, Betts MR, Freeman GJ, Vignali DA, Wherry EJ. 2009. Coregulation of CD8+ T cell exhaustion by multiple inhibitory receptors during chronic viral infection. Nat Immunol 10:29–37. https://doi.org/10.1038/ni.1679.

69. Mueller SN, Ahmed R. 2009. High antigen levels are the cause of T cell exhaustion during chronic viral infection. Proc Natl Acad Sci U S A 106:8623–8628. https://doi.org/10.1073/pnas.0809818106.

70. Chentoufi AA, Kritzer E, Tran MV, Dasgupta G, Lim CH, Yu DC, Afifi RE, Jiang X, Carpenter D, Osorio N, Hsiang C, Nesburn AB, Wechsler SL, BenMohamed L. 2011. The herpes simplex virus 1 latency-associated transcript promotes functional exhaustion of virus-specific CD8+ T cells in latently infected trigeminal ganglia: a novel immune evasion mechanism. J Virol 85:9127–9138. https://doi.org/10.1128/JVI.00587-11.

71. Wherry EJ, Ha SJ, Kaech SM, Haining WN, Sarkar S, Kalia V, Subramaniam S, Blattman JN, Barber DL, Ahmed R. 2007. Molecular signature of CD8+ T cell exhaustion during chronic viral infection. Immunity 27:670–684. https://doi.org/10.1016/j.immuni.2007.09.006.

72. Barber DL, Wherry EJ, Masopust D, Zhu B, Allison JP, Sharpe AH, Freeman GJ, Ahmed R. 2006. Restoring function in exhausted CD8 T cells during chronic viral infection. Nature 439:682–687. https://doi.org/10.1038/nature04444.

73. Chew GM, Fujita T, Webb GM, Burwitz BJ, Wu HL, Reed JS, Hammond KB, Clayton KL, Ishii N, Abdel-Mohsen M, Liegler T, Mitchell BI, Hecht FM, Ostrowski M, Shikuma CM, Hansen SG, Maurer M, Korman AJ, Deeks SG, Sacha JB, Ndhlovu LC. 2016. TIGIT marks exhausted T cells, correlates with disease progression, and serves as a target for immune restoration in HIV and SIV infection. PLoS Pathog 12:e1005349. https://doi.org/10.1371/journal.ppat.1005349.

74. Chentoufi AA, Dasgupta G, Christensen ND, Hu J, Choudhury ZS, Azeem A, Jester JV, Nesburn AB, Wechsler SL, BenMohamed L. 2010. A novel HLA (HLA-A*0201) transgenic rabbit model for preclinical evaluation of human CD8+ T cell epitope-based vaccines against ocular herpes. J Immunol 184:2561–2571. https://doi.org/10.4049/jimmunol.0902322.

75. Chentoufi AA, Dervillez X, Dasgupta G, Nguyen C, Kabbara KW, Jiang X, Nesburn AB, Wechsler SL, BenMohamed L. 2012. The herpes simplex virus type 1 latency-associated transcript inhibits phenotypic and functional maturation of dendritic cells. Viral Immunol 25:204–215. https://doi.org/10.1089/vim.2011.0091.

76. Garon EB, Rizvi NA, Hui R, Leighl N, Balmanoukian AS, Eder JP, Patnaik A, Aggarwal C, Gubens M, Horn L, Carcereny E, Ahn MJ, Felip E, Lee JS, Hellmann MD, Hamid O, Goldman JW, Soria JC, Dolled-Filhart M, Rutledge RZ, Zhang J, Lunceford JK, Rangwala R, Lubiniecki GM, Roach C, Emancipator K, Gandhi L, KEYNOTE-001 Investigators. 2015. Pembrolizumab for the treatment of non–small-cell lung cancer. N Engl J Med 372:2018–2028. https://doi.org/10.1056/NEJMoa1501824.

77. Rizvi NA, Hellmann MD, Snyder A, Kvistborg P, Makarov V, Havel JJ, Lee W, Yuan J, Wong P, Ho TS, Miller ML, Rekhtman N, Moreira AL, Ibrahim F, Bruggeman C, Gasmi B, Zappasodi R, Maeda Y, Sander C, Garon EB, Merghoub T, Wolchok JD, Schumacher TN, Chan TA. 2015. Mutational landscape determines sensitivity to PD-1 blockade in non-small cell lung cancer. Science 348:124–128. https://doi.org/10.1126/science.aaa1348.

78. Rizvi NA, Mazieres J, Planchard D, Stinchcombe TE, Dy GK, Antonia SJ, Horn L, Lena H, Minenza E, Mennecier B, Otterson GA, Campos LT, Gandara DR, Levy BP, Nair SG, Zalcman G, Wolf J, Souquet PJ, Baldini E, Cappuzzo F, Chouaid C, Dowlati A, Sanborn R, Lopez-Chavez A, Grohe C, Huber RM, Harbison CT, Baudelet C, Lestini BJ, Ramalingam SS. 2015. Activity and safety of nivolumab, an anti-PD-1 immune checkpoint inhibitor, for patients with advanced, refractory squamous non-small-cell lung cancer (CheckMate 063): a phase 2, single-arm trial. Lancet Oncol 16:257–265. https://doi.org/10.1016/S1470-2045(15)70054-9.

79. National Research Council. 2011. Guide for the care and use of laboratory animals, 8th ed. National Academies Press, Washington, DC.

80. Srivastava R, Khan AA, Garg S, Syed SA, Furness JN, Vahed H, Pham T, Yu HT, Nesburn AB, BenMohamed L. 2017. Human asymptomatic epitopes identified from the herpes simplex virus tegument protein VP13/14 (UL47) preferentially recall polyfunctional effector memory CD44^high CD62L^low CD8+ T_EM cells and protect "humanized" HLA-A*02:01 transgenic mice against ocular herpes. J Virol 91:e01793-16. https://doi.org/10.1128/JVI.01793-16.

81. Looker KJ, Garnett GP, Schmid GP. 2008. An estimate of the global prevalence and incidence of herpes simplex virus type 2 infection. Bull World Health Organ 86:805–812. https://doi.org/10.2471/BLT.07.046128.

82. Nesburn AB, BenMohamed L. 2017. A tribute to Professor Steven L. Wechsler (1948–2016): the man and the scientist. Curr Eye Res 42: 161–162. https://doi.org/10.1080/02713683.2016.1252405.